ELSEVIER

Fuel Processing Technology 86 (2005) 1707–1743

FUEL PROCESSING TECHNOLOGY

www.elsevier.com/locate/fuproc

Review

Review—calcination and carbonation of limestone during thermal cycling for CO_2 sequestration

B.R. Stanmore, P. Gilot*

Laboratoire Gestion des Risques et Environnement, 25 rue de Chemnitz, 68200 Mulhouse, France

Received 1 July 2004; accepted 1 January 2005

Abstract

Some aspects of using lime from limestone to sequester CO_2 from combustion systems are examined in this review of the literature. A typical sequestration technology would consist of two circulating fluidised beds, one operated in the temperature range 600–700 °C and acting as a carbonator, and the other in the temperature range 750–950 °C acting as a cracker. The processes involved in calcination, sintering, and carbonation are summarised, including the relative rates of reaction. The physical properties of the calcined products after sintering and reaction are reviewed. The loss of active calcium due to the competitive formation of sulphates and other calcium compounds is noted. Prolonged residence times in fluidised bed systems will lead to extensive loss of surface area and porosity in the particles. The likely extent of particle fragmentation is discussed, and some cost figures for avoided CO_2 emissions from power generation systems are presented. The need for a realistic model of the processes taking place in the particles is emphasised.

Keywords: Calcination; Carbonation; Limestone; CO_2 sequestration; Sulphation

Contents

* Corresponding author. Tel.: +33 3 89 32 76 57; fax: +33 3 89 32 76 61.
E-mail address: Patrick.gilot@uha.fr (P. Gilot).

0378-3820/$ - see front matter © 2005 Elsevier B.V. All rights reserved.
doi:10.1016/j.fuproc.2005.01.023

1. Introduction

There is considerable pressure on industries which rely on combustion to minimise their emissions of carbon dioxide. This has led to proposals to capture the CO_2 in the combustion gases, and then release it separately in a concentrated stream, which is able to be fixed more efficiently and economically than the dilute combustion gas [1]. One vehicle being proposed to accomplish this separation is lime, i.e. CaO, which will be carbonated to $CaCO_3$ at a lower temperature in the flue gas, removed from the process (carbonation) vessel, and then decomposed in a separate (cracker) vessel at a higher temperature. The regenerated lime would then be returned to the carbonator [2,3].

This process can be economical because the raw material is limestone and circulating fluidised beds are suitable process vessels. This review will be restricted to limestone, although dolomite $CaMg(CO_3)_2$ and dolostones, which are mixtures of calcium and magnesium carbonates can also act as sorbents. Magnesium carbonate decomposes at a much lower temperature than calcium carbonate, so that in the

combustion systems envisaged for this application, it would not contribute to CO_2 capture. Any $MgCO_3$ present in the limestone will act as inert MgO during the CO_2 sequestration process.

The addition of limestone at a high temperature to a contacting vessel in which the flue gases contain carbon dioxide, water vapour and sulphur dioxide sets in train a series of interlinked reactions. The fresh limestone is calcined to lime (CaO), which can then react with both CO_2 (carbonation) and SO_2 (sulphation). After the formation of the calcine, the open structure of the lime initially formed is modified by sintering. The progress of these reactions, which include calcination/carbonation, sintering, sulphation/desulphation and particle fragmentation, depends on the nature of the limestone and the conditions inside the process vessel.

All of these processes have been examined in isolation, but in practice, a charge of sorbent in a circulating fluidised bed (CFB) will have experienced a number of cycles in which all the processes are occuring simultaneously. In particular, the presence of other calcium compounds (OCCs) and any sulphation of the lime will decrease the amount of active CaO available for carbonation. In addition, its formation will tend to block access to the interior of the pores. The regeneration step will need to decompose $CaSO_4$ as well as $CaCO_3$. Any mathematical model proposed to simulate the operation of CFBs with limestone addition will need to incorporate all of these steps.

2. Calcination

The calcination reaction is endothermic

$$CaCO_3 \rightarrow CaO + CO_2 \quad \Delta H = +182.1 \text{ kJ mol}^{-1}$$

which means that the forward reaction is favoured by higher temperatures. The reaction will proceed only if the partial pressure of CO_2 in the gas above the solid surface is less than the decomposition pressure of the $CaCO_3$. The latter pressure is determined by equilibrium thermodynamic considerations. A typical expression for equilibrium decomposition pressure P_{eq} quoted by Silcox et al. [4] is:

$$P_{eq} = 4.137 \times 10^7 \exp\left(-\frac{20474}{T}\right) \text{ atm} \tag{1}$$

Fig. 1 plots three of the expressions listed in the literature; the agreement is good except at lower temperatures.

In a bulky sample, e.g. a large particle or a packed bed, decomposition may be inhibited because of local high concentrations of CO_2 held in the pores of a particle, or in the interstices of a bed. In some experimental procedures, decomposition is prevented from commencing at high temperature by charging the reaction vessel with pure CO_2, so that the decomposition pressure is exceeded. True decomposition rates can be measured only under differential conditions, which ensure that the concentration of CO_2 is controlled or known.

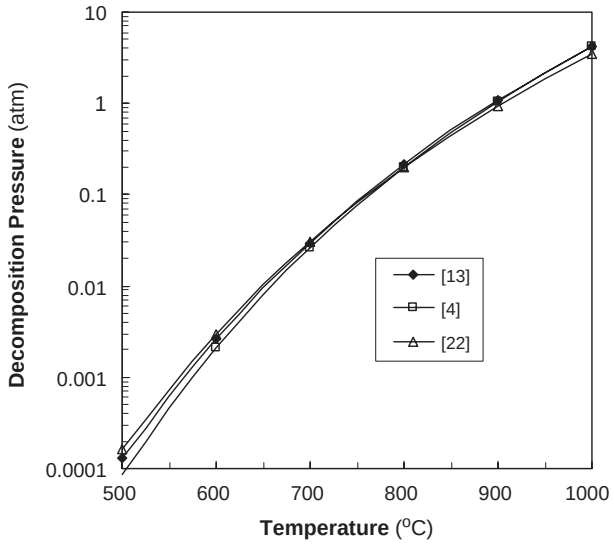

Fig. 1. Decomposition pressure of carbon dioxide over calcium carbonate.

2.1. The properties of limestones and their calcines

Commercial limestone rock generally consists of over 90% calcium carbonate and contains from 3 to 35% voids ($\varepsilon = 0.03$–0.35). This voidage is almost exclusively in the form of larger pores, with few micropores, so that the specific surface area ranges from 1 to 10 $m^2\ g^{-1}$. Most limestones occur as calcite, and in the absence of significant impurities, do not shrink upon calcination [5]. It is found that the ability of limestones capture sulphur can vary from location to location in the same mine, and no overall correlating description for efficacity has been identified. From his study of 25 limestones, Trikkel [6] notes that impurities such as iron and aluminium oxides tend to lead to lower surface areas in both the limestones and their calcines. He also found that the mass loss versus time curves in a temperature-ramped TGA were the same shape for different limestones under the same conditions, but displaced in temperature by 10 to 15 K. Geologically younger stone (e.g. chalk) exhibits greater initial porosity and greater sorption capacity for sulphur dioxide [7].

Borgwardt [8] has shown that if the micrograins are considered to consist of a face-centered array of uniform spheres ($\varepsilon = 0.48$, $S_o = 104\ m^2\ g^{-1}$), they must be 17.4 nm in diameter. The apparent pore diameter of the surrounding voids will be approximately 4 nm. In fact the grains are smaller than this, and are found in clusters which have larger equivalent pore diameters between them. From his study on sintering, Borgwardt concluded that each cluster must contain on average 125 grains.

When calcination takes place, the product calcium oxide weighs only 56% of the parent carbonate. Since the relative molar volumes are 36.9 $cm^3\ mol^{-1}$ for $CaCO_3$ and 16.9 $cm^3\ mol^{-1}$ for CaO, if there is negligible particle shrinkage, the porosity of the product from a pure non-porous carbonate will increase to a theoretical value of 0.55. Hence a lime may have a porosity greater than 0.6. For maximum adsorption efficiency, care must be taken

on the one hand to ensure that calcination is complete, and on the other that the CaO grains formed do not sinter after formation.

Table 1 shows the measured values for some surface areas and porosities of calcined solid as reported by various researchers. Krishnan and Sotirchos [9] report on the difficulties encountered in trying to measure the porosity of calcined limestone by means of mercury porosimetry and gas adsorption techniques, so that there may be some difficulty in reconciling the values. The specific surface area of nascent CaO (i.e. product which has not suffered sintering) S_o is around 104 $m^2\ g^{-1}$ [8]. From a perusal of the data of Table 1, it must be concluded that most of the CaO products have suffered some sintering, as they exhibit surface areas which are significantly lower than the nascent values.

Barker [10] repeatedly calcined 10 μm particles of AR $CaCO_3$ and then recarbonated the product. Both the limestone and the recarbonated calcines showed no porosity, with surface areas of 0.46 and 0.34 $m^2\ g^{-1}$ respectively. The calcine area after the first calcination was 28.7 $m^2\ g^{-1}$. The experimentally measured activation energy for this process ($\approx$100 kJ mol^{-1}) was regarded as related to the migration of atoms associated with the change from carbonate to oxide ions. The pore size distribution measured by mercury porosimetry showed a peak between 10 and 100 nm.

The porosities of calcines formed from seven European limestones which had been treated at 850 °C were measured by mercury porosimetry by Adánez et al. [11]. Most, like Blanca limestone gave unimodal pore size distributions around 30 to 40 nm. Two others, from Sástago and Alborge displayed widely distributed pore sizes, ranging from 40 nm to 10 μm. From the equivalent surface area of a calcine, Borgwardt et al. [12] calculated the grains to be 11 nm in size. After examining micrographs of the CaO obtained from the vacuum calcination of calcium hydroxide at 980 °C,

Table 1
Some properties of CaO prepared by calcining limestone

Limestone	% $CaCO_3$	Calcination temp. (°C)	Calcine surface area ($m^2\ g^{-1}$)	Calcine porosity	Reference
Blanca	97.1	900	19	0.56	[13]
Mequinenza	95.8		19.4	0.68	
Massici	96.8	850	–	0.37	[54]
Unspecified	96.1	780	–	–	[21]
Fredonia White	96	700	104	–	[12]
Unspecified	–	870	–	0.47–0.60	[73]
Greer Limestone	>95	750	56	0.51	[9]
		850	45	0.51	
Georgia Marble	>95	850	52	0.46	
Unspecified	–	750	37	–	[83]
		850	25		
		900	6.6		
Fredonia Valley	–	600	87	–	[8]
		800	75		
		950	70		

Borgwardt reports that the structure was in the form of micrograins of size 5–10 nm. Other authors report similar results. The micrographs presented by García-Labiano et al. [13], indicate that these grains are aggregated into clusters of about 1 μm in mean size.

A limestone from Strassburg (USA), which consisted of 97.0% $CaCO_3$, was calcined in order to study the fracture of sulphate layers [14]. The material was calcined in air for 90 min at 870 °C, and some was then further sintered in air for 24h at 1300 °C. The calcined samples were regarded as 'unsintered', despite having a BET area of only 1.5 $m^2\ g^{-1}$. The measured pore size distribution showed two maxima, one around 3–5 nm and the second at 60–80 nm. The SEM micrograph of the unsintered surface reveals a network of fused grains about 200 nm in width, separated by the larger pores. The appearance was similar to that presented by García-Labiano et al. [13] for a 'semi-sintered' sample, and by Laursen et al. [15]. The area of the 'sintered' Strassburg samples was about 0.38 $m^2\ g^{-1}$. By contrast, the appearance of the sintered material showed that the grains had fused into large rounded, non-porous globules about 2–5 μm in diameter. These were joined at necks of almost the same thickness as the spherical grains. As a result, the effective pore diameters are very large, of the order of microns.

A total of nine limestones was collected from around the world and subjected to sintering and sulphation by Laursen et al. [15]. The sintering was carried out on 212 to 355 μm particles for 3 h at 850 °C under nitrogen. The grain sizes reported range from <0.1 to 0.6–0.8 μm, with most in 0.2–0.5 μm range. They have a rounded surface morphology, similar to other SEM micrographs. The porosity was allocated visually to fractures and micro and macropores. The micropores are irregular and inter-connected voids, which ranged from virtually non-visible to 3 μm in the more reactive samples. Macropores, which seen as irregular voids separating groups of grains, were only observed in two samples, with typical widths of 0.5 μm.

2.1.1. Comment

From the studies mentioned above, it is apparent that an initial calcination of pure limestone under process conditions will involve some sintering, leading to the production of a semi-fused mass consisting of 200–500 nm grains separated by pores of 100 nm width. The porosity will still be significant. Further thermal exposure in the process will lead to a decrease in both porosity and surface area as a result of further sintering, which will be compounded by pore closure due to carbonation and/or sulphation. After several hours of residence time in the circulating systems, it can be anticipated that the particles will exhibit a highly fused nodular surface.

2.2. The kinetics of calcination

Evaluation of the kinetics of calcination is complicated by

(1) CO_2 concentration, which inhibits the reaction,
(2) particle size, which may introduce both thermal and mass transfer limitations, and
(3) catalysis/inhibition by impurities.

Regarding point (3), Huang and Daugherty [16,17] found that V_2O_5 and fly ash inhibit calcination, that Al_2O_3 and CaO have no effect, but that Li_2CO_3 accelerates the process.

Barker [10] found that complete calcination was rapidly achieved, i.e. in less than 1 min. At 1000 °C and 1 mbar pressure, 90% calcination was achieved in less than 2.5 s [18]. The inherent kinetics of the calcination reaction under zero partial pressure of CO_2 have been extensively measured. To accommodate points (1) and (2), a model is needed to interpret the experimental data. The usual units for rate are mol m^{-2} s^{-1}, with the area basis generally being the reaction front area. This must be established by a suitable model for each case.

A plot of a number of rate equations presented in the literature is given as Fig. 2 in the form of an Arrhenius diagram. The disagreement probably reflects the different models used for surface area, e.g. Blanca limestone was analysed by García-Labiano et al. [13] with a Shrinking Core Model (SCM) and Mequinenza limestone with a Changing Grain Size Model (CGSM). Other models were used in the various analyses of experimental data, which were not necessarily free from transport resistances.

By using small (1 μm) particles in which transport effects are negligible, Borgwardt et al. [12] report a decomposition rate for 670 °C:

$$R_c = 2.5 \times 10^{-4} \quad \text{mol m}^{-2}\ \text{s}^{-1} \tag{2}$$

with an activation energy of 49 kJ mol^{-1}. Dennis and Hayhurst [19] measured the calcination rates in a fluidised bed at temperatures between 800 and 975 °C. They found

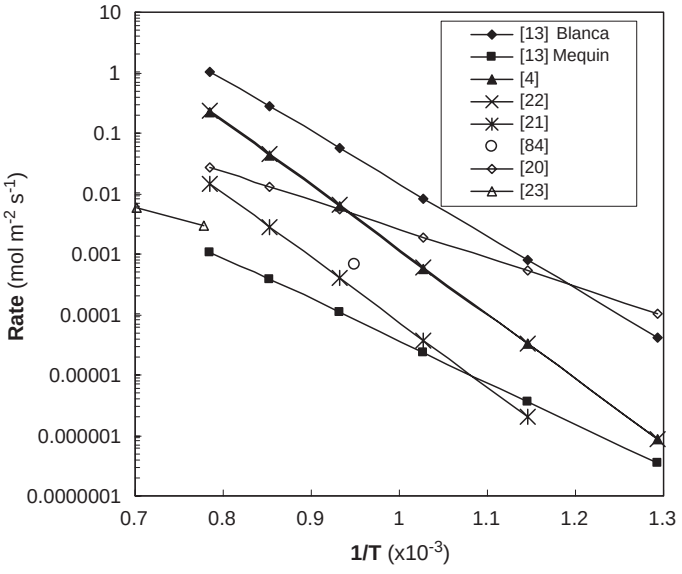

Fig. 2. The influence of temperature on the calcination rate of limestone, measured by a number of investigators.

no influence of temperature in this range, which implies zero associated activation energy. The calcination rate of limestone was given by Silcox et al. [4] as

$$R_c = k_D\left(P_{eq} - P_i\right) \quad \text{mol m}^{-2}\ \text{s}^{-1} \tag{3}$$

where P_i is the partial pressure of CO_2 at the reaction surface and

$$k_D = 1.22\exp(-4026/T) \quad \text{mol m}^{-2}\ \text{s}^{-1}\ \text{atm}^{-1} \tag{4}$$

This expression also appears to have a low activation energy (33.4 kJ mol^{-1}), but when multiplied by the decomposition pressure P_{eq}, it exhibits a similar temperature dependence to the findings of other researchers. The result for zero partial pressure P_i of CO_2 is shown in Fig. 2, together with the results for the other correlations discussed here.

A model based on a modified shrinking core approach was developed by Milne et al. [20] and applied to limestone. The modification consisted in adjusting the rate kinetics for calcination by incorporating the mean grain size d_o, taken to the 0.6 power. Thus the conversion X is given by a modified expression involving a rate coefficient k ($\text{m}^{0.6}\ \text{s}^{-1}$):

$$X = 1 - \left(1 - \frac{k}{d_o^{0.6}}t\right)^3 \tag{5}$$

The experimentally determined modification has the effect of spreading the reaction front and allowing for sintering. The value of k is given by

$$k = 10.303\exp(-10,980/T) \quad \text{m}^{0.6}\ \text{s}^{-1} \tag{6}$$

In order to give an expression which is comparable to the other rate equations of Fig. 2, one must include both a grain size, radius=r_o and the specific surface area:

$$k_c = \frac{\rho_c}{M}\frac{k r_o^{0.4}}{2^{0.6}} \quad \text{mol m}^{-2}\ \text{s}^{-1} \tag{7}$$

where ρ_c is the density of the limestone and M is the molecular mass of the reactant. The grain size was calculated from

$$r_o = 3/(\rho_c S_o) \tag{8}$$

With the surface area taken as 20 $\text{m}^2\ \text{g}^{-1}$ and the density as 2700 kg m^{-3}, the result is shown in Fig. 2. It falls among the other results, but shows a much lower activation energy.

An investigation undertaken by Khinast et al. [21] used only the single temperature of 780 °C. In this case

$$R_c = k_c f(CO_2) = 2.027 \times 10^{-4} f(CO_2) \quad \text{mol m}^{-2}\ \text{s}^{-1} \tag{9}$$

where $f(CO_2)$ is a function involving the concentration of CO_2. Hu and Scaroni [22] examined the calcination of 6–90 μm limestone particles in a drop tube furnace and found

significant resistances due to mass and heat transfer. The inherent reaction rate of calcination was deduced by means of their model to be

$$R_c = -k_c S f(CO_2) \quad \text{mol s}^{-1} \tag{10}$$

where

$$k_c = 6.078 \times 10^7 \exp(-205,000/RT) \quad \text{mol m}^{-2}\ \text{s}^{-1} \tag{11}$$

During a similar investigation, two models were developed to extract inherent calcination kinetics from measurements with 0.4 to 2.0 mm particles treated by isothermal thermogravimetric analysis [13]. The two approaches were deemed necessary after an SEM examination of partially calcined particles. The CGSM was applied Mequinenza limestone in which extent of calcination varied continuously with radial position. In contrast, the SCM was deemed appropriate for Blanca limestone. The rate expression given for the CGSM and SCM is

$$R_c = k_c S_o (r/r_o)^2 f(CO_2) \tag{12}$$

where k_c is the fundamental kinetic relationship and r is the radius of the reaction front. The plots in Fig. 2 of the Arrhenius relationship of k_c found for these two limestones exhibit a wide divergence. The difference probably reflects the model used, as the SCM adopted for Blanca limestone will give a much lower reaction area, and hence a higher rate.

The decomposition of calcium hydroxide rather than calcium carbonate has also been examined. For example, 12.5 μm particles of $Ca(OH)_2$ were calcined in a nitrogen atmosphere at two temperatures by Mai and Edgar [23]. Using the initial surface area of 11.5 $m^2\ g^{-1}$ as the reference, they found the conversion rate to be 0.22 g $m^{-2}\ s^{-1}$ at 1275 K and 0.43 g $m^{-2}\ s^{-1}$ at 1425 K. These values represent data at the higher temperature end of those shown in Fig. 2. The kinetics of calcination of 3.6 μm $Ca(OH)_2$ particles under nitrogen were studied by Ghosh-Dastidar et al. [24], with the aim of producing a highly reactive SO_2 sorbent. Conversion was rapid for the first 100 ms at 900 °C, but then slowed. Conversion was almost complete after 200 ms at 1100 °C. The activation energy was reported to be 95 kJ mol^{-1}.

2.2.1. The effect of carbon dioxide and water vapour on calcination rate

The effect on the kinetic rate of carbon dioxide in the gas phase, i.e. the nature of the function $f(CO_2)$, is the subject of some disagreement. All researchers found that the presence of CO_2 inhibited the calcination reaction, but the form of dependence is uncertain. Identifying the relationship is complicated by the fact that the calcination will be influenced by the local CO_2 concentration, namely that at the reaction surface P_i, and not the bulk gas concentration P_b. In most cases the value of P_i cannot be directly measured, but must be inferred from a model. As mentioned above, there are various approaches to interpreting the reaction interface, and this will influence the resulting CO_2 dependence.

The rate of calcination R_c is given by Dennis and Hayhurst [25] as

$$R_c = k_c\left(P_{eq} - P_i - \text{const} \times P\right) \quad \text{mol m}^{-2}\ \text{s}^{-1} \tag{13}$$

where P is the total pressure. They could not explain the third term, which is an effective mole fraction for CO_2. In a similar approach, Silcox et al. [4] took a shrinking core model, and give the calcination rate as

$$R_c = k_c\left(P_{eq} - P_i\right) \quad \text{mol m}^{-2}\ \text{s}^{-1} \tag{14}$$

Following the findings of Darroudi and Searcy [26], Hu and Scaroni [22] propose that

$$k_c = k_c' \quad \text{mol m}^{-2}\ \text{s}^{-1} \quad P_i<10^{-2}P_{eq} \tag{15}$$

$$k_c = k_c'\left(P_{eq} - P_i\right)/P_{eq} \quad \text{mol m}^{-2}\ \text{s}^{-1} \quad 10^{-2}P_{eq}<P_i<P_{eq} \tag{16}$$

where

$$k_c' = 6.078 \times 10^7 \exp(-205000/RT) \quad \text{mol m}^{-2}\ \text{s}^{-1}. \tag{17}$$

Eqs. (14) and (16) conform to the findings of Barker [10] that CO_2 concentration has no influence on rate if it is well below the decomposition pressure.

As noted above, Silcox et al. [4] incorporated the CO_2 effect into the rate expression as a separate term. From an analysis of experimental measurements, Khinast et al. [21] adopted an exponential function for $f(CO_2)$. Then

$$R_c = k_c \exp\left(-11.92P_i/P_{eq}\right) \quad \text{mol m}^{-2}\ \text{s}^{-1} \tag{18}$$

In contrast, García-Labiano et al. [13] tested the above types of empirical relationship to evaluate $f(CO_2)$, but finally preferred an approach based on adsorption theory. The Freundlich relation worked better than a modified Langmuir expression

$$R_c = k_c S_o(1-\theta)\left(1 - P_i/P_{eq}\right) \quad \text{mol m}^{-3}\ \text{s}^{-1} \tag{19}$$

where $\theta = cP_i^{1/2}$ and $c = c_o \exp(-E_a/RT)$. For Blanca limestone they give $E_c = 166$ kJ mol^{-1}, $k_o = 6.7 \times 10^6$, $c_o = 1.8 \times 10^{-7}$ Pa$^{-1/2}$ and $E_a = -93$ kJ mol^{-1}; the equivalent values found for Mequinenza limestone were $E_c = 131$ kJ mol^{-1}, $k_o = 2.54 \times 10^2$, $c_o = 3.7 \times 10^{-7}$ Pa$^{-1/2}$ and $E_a = -90$ kJ mol^{-1} respectively.

In their study of calcite decomposition, Wang and Thompson [27] observed the progress of the reaction by means of dynamic X-ray diffraction to identify the solid phases. The calcite particles, which were 1.87 μm in size, were heated in a TGA with both steam and CO_2 in the gas phase. They found that both water and CO_2 molecules were adsorbed onto the $CaCO_3$ surface at 300 °C, with water more strongly held, and able to displace CO_2. At that temperature, the adsorptive capacity was 0.0092 mole of water per g of calcite. They fitted the behaviour of the system with a quantitative Langmuir–Hinshelwood model which allowed the kinetics to be established. For both gases, the rate of decomposition was accelerated, but the data are predicated on the Langmuir–Hinshelwood model and difficult to apply independently. They speculate that the adsorbed H_2O

molecules weaken the bond between CaO and CO_2, and thus catalyse the decomposition of the crystal lattice.

A recent investigation by Agnew et al. [28] studied the decomposition and sintering of 75–106 μm particles of two limestones, Omyacarb (Spain) and Derbyshire (UK). The gas environment consisted of 13.0% H_2O, 6.5% CO_2, 2.1% O_2, with the remainder nitrogen. The kinetic constants measured, based on the surface areas of the parent limestones (0.3 $m^2\ g^{-1}$ in each case), were 799 $\exp(-11{,}900/T)$ and 77.2 $\exp(-8680/T)$ mol $m^{-2}\ s^{-1}$ respectively. These rates are higher than those under an inert gas such as N_2 as typified by the data of Khinast et al. [21], see Fig. 3. It appears that H_2O and perhaps CO_2 catalyse the decomposition.

The kinetic constants for the calcination of two types of $Ca(OH)_2$ derived from Omyacarb limestone in an atmosphere of 15% CO_2 and 7% H_2O in nitrogen are given by Adánez et al. [11] as

$$k_c = 19.1\exp(-4374/T) \quad \text{mol m}^{-2}\ \text{s}^{-1} \tag{20}$$

and

$$k_c = 53.8\exp(-6033/T) \quad \text{mol m}^{-2}\ \text{s}^{-1} \tag{21}$$

These rates are much higher than the equivalent rates for limestone.

2.2.2. The effect of particle size on calcination rate

Ye et al. [29] do not recommend fine grinding below 5 μm due to the cost of grinding and the concommitant destruction of pore volume. On the other hand, a decrease below 1–2 μm is said to have only a limited effect on conversion, even though pore diffusion limitations are entirely absent. Cheng et al. [30] claim that the decomposition of 14 μm particles at 1000 °C is controlled by the chemical reaction. The calcination rates of 3.9 μm

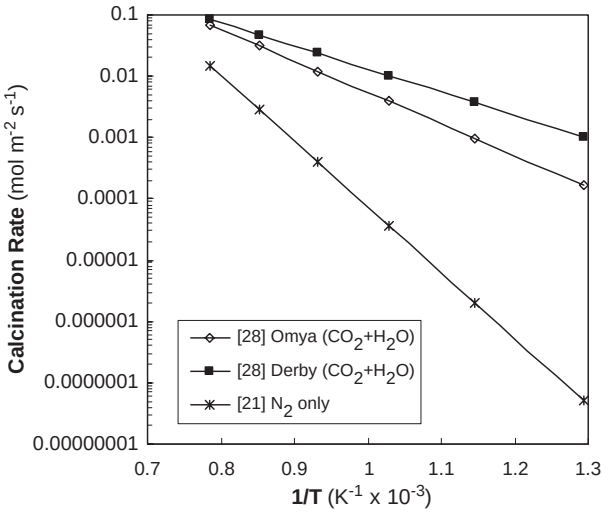

Fig. 3. The influence of an atmosphere containing CO_2 and H_2O on the calcination rate of limestone.

limestone particles at 1080 °C were found to be the same as those of $Ca(OH)_2$ particles of the same size [31]. Since $Ca(OH)_2$ is known to decompose readily, it was concluded that no diffusion limitations were present for CO_2 escape at that particle size. Trikkel [6] found significant differences in decomposition rates in a TGA between particles in the range 0–45 μm and those in the range 0.63–1 mm.

Borgwardt [12] considered that limestone particles <90 μm in diameter would calcine uniformly throughout. In contrast, for this size of particle most other researches resort to a model such as a SCM for analysing the reaction kinetics. Hu and Scaroni [22] detected significant effects from particle size when using 63 μm limestone particles. They came to this conclusion for two reasons:

1. some SEM micrographs of treated particles showed a gradation in extent of calcination from the outer surface to the centre, and
2. the model that they developed indicated that with the inherent reaction kinetics adopted (Eqs. (10) and (11)), such gradations would exist.

Fig. 4 shows the predicted profile of extent of calcination with radius, 0.1 s after the injection of a 63 μm limestone particle into nitrogen at 1473 K. The local value of conversion ranged from 85% at the surface to 29% at the centre.

Murthy et al. [32] investigated the calcination of compacts of 3 μm $CaCO_3$ powder, which had been compressed to a porosity of 0.63 in cylinders of 8.95, 11.95 and 17 mm diameter. A model of mass and heat transfer was applied and found to adequately predict performance. Some kinetic data are given, but they apply to the overall compact and not to the inherent reaction. The values are orders of magnitude lower than those presented in Fig. 2, indicating severe transport limitations in such large particles. An activation energy of 167 kJ mol^{-1} is reported.

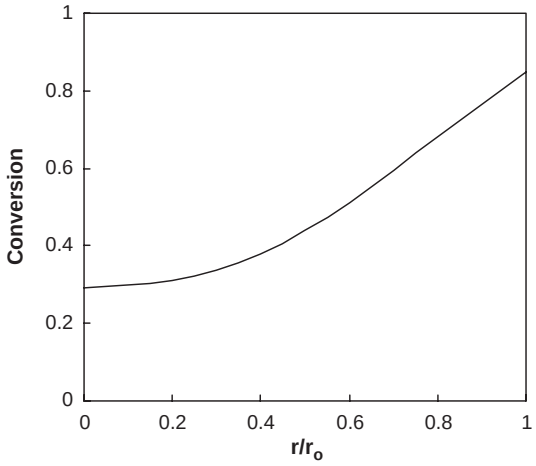

Fig. 4. The predicted variation in the extent of calcination (X) with dimensionless radius for a 63 μm limestone sphere after 0.1s exposure to N_2 at 1200 °C [22].

3. Sintering

In practice, the conditions in a commercial fluidised bed will permit sintering, which will decrease both the porosity and surface area of the adsorbent. Sintering is favoured both by high temperatures and time at temperature, and is accelerated by the presence of CO_2 and H_2O. The decrease in carbonation capacity reported during cycling of calcination/carbonation reactions is attributed to sintering and pore closure [33].

During sintering, necks develop between adjacent grains and continue to grow. The material for this growth is supplied from the rest of the grain, so that the distance between grain centres is diminished. This causes both the voidage and the surface area to decrease. However, a macropore network also develops, in which the pores are estimated to have a mean diameter of 17 nm when sintering is complete. The surface area can decrease to almost zero if sintering is continued at 1050 °C. The rate as well as the extent of sintering is affected by the presence of water vapour and carbon dioxide in the gas phase.

3.1. Sintering rates

Borgwardt [9] fitted a sintering relationship developed by German and Munir [34] to his experimental data, which describes the change in surface area S (as measured by nitrogen BET area) with sintering time:

$$\left(\frac{S_o - S}{S_o}\right)^{\gamma} = K_s t \tag{22}$$

where K_s is a rate constant for the temperature (min^{-1}) and t is time. For a significant number of experimental conditions in an inert gas atmosphere (no CO_2 or H_2O), the exponent γ was found to lie in the vicinity of 2.7, which is consistent with the mechanism of lattice diffusion.

The rate constant K_s was well-described by an Arrhenius type of relationship. The rates for sintering CaO prepared from limestone, pure $CaCO_3$ and pure $Ca(OH)_2$ showed different rates and different activation energies. The highest rate for CaO prepared from limestone compared to pure $CaCO_3$ (by a factor of at least 10) was attributed to the presence of foreign ions in the natural rock. These ions produce defects in the crystal lattice which encourage lattice diffusion. The rate for CaO prepared from pure $Ca(OH)_2$ was higher again by a factor of 10. The reason proposed for this was its lower porosity (0.40 vs. 0.48), which implies closer contact between grains and a greater propensity for neck formation.

This approach was then extended by Borgwardt [35] in a study of the effect of CO_2 and H_2O on the rate of sintering, as measured by BET area. Both cause an acceleration of the process, with water vapour being more active. It was found that the values of both γ and K_s in Eq. (22) had to be significantly increased in order to describe the progress of sintering under the effect of CO_2 and H_2O. The increase in γ implies that other methods of diffusion besides lattice diffusion become operative.

Borgwardt concludes that both gases catalyse the decomposition of $CaCO_3$, and their effects are additive. He gives for water

$$\ln\gamma_{H_2O} = 0.00262\ T + (\ln P_{H_2O} - 1.39)/11.1 \tag{23}$$

and for CO_2

$$\ln\gamma_{CO_2} = 0.0024\ T + (\ln\ P_{CO_2} - 1.948)/44.9 \tag{24}$$

For the kinetic coefficient with CO_2 present

$$\ln K_s = 1.485 + 0.558\ln P_{CO_2} - 11660/T\ \text{min}^{-1} \tag{25}$$

The three expressions above, for γ and K_s give totally unrealistic values when the appropriate data are supplied, and there must be errors in their formulation. Accordingly the raw data from references of Borgwardt were crudely fitted by the authors. It was found that the rate expression Eq. (25) is actually for water vapour, and a separate correlation was required for carbon dioxide. The recommended values are

$$\gamma_{H_2O} = 10.5(1.52\ln P_{H_2O} - 1.9)\exp(-2520/T) \tag{26}$$

$$\gamma_{CO_2} = 44.1(0.80\ln P_{CO_2} - 1.0)\exp(-4140/T) \tag{27}$$

and

$$\ln\ K_{sC} = 18.5 + 0.558\ \ln P_{CO_2} - 30000/T\ \text{min}^{-1} \tag{28}$$

$$\ln K_{sH} = 1.485 + 0.558\ \ln P_{H_2O} - 11660/T\ \text{min}^{-1} \tag{29}$$

where P_{H_2O} and P_{CO_2} are in Pascals. The revised values were tested in all the original data and were found to be satisfactory. When both CO_2 and H_2O are present, Borgwardt gives

$$\gamma_{CO_2+H_2O} = 0.376\left(\gamma_{CO_2} + \gamma_{H_2O}\right) + 8.8 \tag{30}$$

An alternative sintering expression first proposed by Nicholson and adopted by Silcox et al. [4] after examining some of Borgwardt's data is

$$\frac{dS}{dt} = -k_s(S - S_{as})^2 \quad \text{m}^2\ \text{g}^{-1}\ \text{s}^{-1} \tag{31}$$

where S_{as} is the asymptotic value of surface area after prolonged sintering. The value of k_s is given by Silcox et al. as

$$k_s = 286\left(\frac{-14500 - 3820P_b^{-0.111}}{T}\right)\ \text{km}^{-2}\ \text{s}^{-1}\ (\text{sic}) \tag{32}$$

where P_b is the partial pressure of CO_2 in atm. Eq. (32) of Silcox also suffers from a number of errors, in this case in a sign and in the units. The expression should probably read

$$k_s = 286\left(\frac{-14500 + 38.2P_b^{-0.111}}{T}\right)\ \text{g}\ \text{m}^{-2}\ \text{s}^{-1} \tag{33}$$

Silcox does not give a means of incorporating the effect of water vapour, and a deficiency of the approach is the prior need to know the asymptotic area value S_{as}.

A direct comparison between the Borgwardt and Silcox approaches to the rates of sintering can be obtained by differentiating Eq. (22) to give an explicit expression for rate

$$\frac{dS}{dt} = -\frac{S_o}{\gamma} K_s^{\frac{1}{\gamma}} t^{-\left(\frac{\gamma-1}{\gamma}\right)} \quad m^2\ g^{-1}\ s^{-1} \tag{34}$$

Then as an example, the initial rates of sintering at (time $t=0$) for a range of temperatures, based on $\gamma=2.7$, $S_o=70\ m^2\ g^{-1}$, $S_{as}=20\ m^2\ g^{-1}$, and at zero concentration of CO_2 are similar, with the Borgwardt expression slightly lower.

The sintering rate of CaO formed from $Ca(OH)_2$ under an atmosphere of nitrogen was measured by Mai and Edgar [23] at 1012 and 1152 °C. Because of the high temperatures involved, it was necessary to model the calcination and shrinkage steps as competing processes. Assuming that the unsintered calcined product area was 70 $m^{-2}\ g^{-1}$, and using the Silcox description of shrinkage (Eq. (31)), they found rates of 0.128 and 2.7 g $m^{-2}\ s^{-1}$ respectively. The corresponding asymptotic areas for shrinkage were 20.2 and 18.1 $m^{-2}\ g^{-1}$. When these are plotted in Fig. 5 as an overall rate of initial change of S, they represent a significant increase over the Borgwardt [8] and Silcox [4] values, and are in fact higher than the rates for sintering catalysed by CO_2 and H_2O [28]. The activation energy between the two values is 327 kJ mol^{-1}. The activation energy reported by Ghosh-Dastidar et al. [24] for the same situation was 236 kJ mol^{-1}.

Some experimental results for sintering were obtained by Agnew et al. [28] for two limestones heated in an atmosphere of 6.5% CO_2, 1.8% O_2, 13.0% H_2O and N_2. Because calcination and sintering occurred simultaneously under the conditions used, they took a

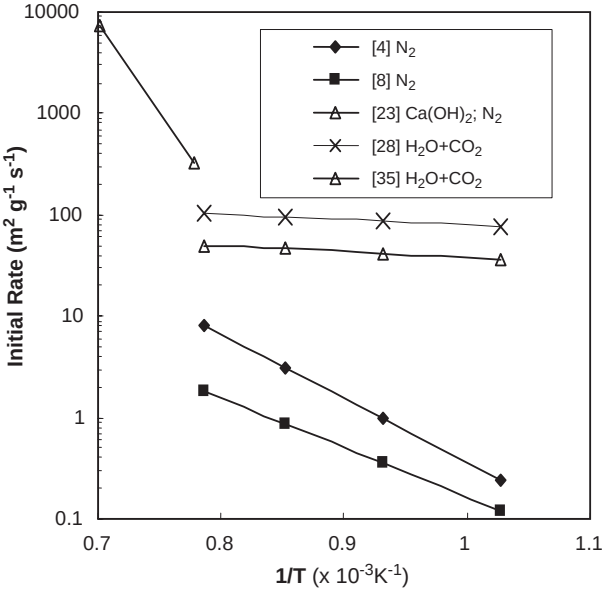

Fig. 5. The influence of an atmosphere containing CO_2 and H_2O on the initial rate of sintering of lime particles.

value of 70 $m^2\ g^{-1}$ for the initial area of the calcine. The Silcox expression, i.e. Eq. (31) was applied to evaluate the kinetic constants. The expression developed for Derbyshire limestone was

$$k_s = 0.164\exp(-1190/T) \quad \text{g m}^{-2}\ \text{s}^{-1} \tag{35}$$

The original units for Eq. (35) were given as kg $m^{-2}\ s^{-1}$, but this gives calculated values of rate which are many orders of magnitude larger than those measured. Although an equivalent expression for Omyacarb limestone was not given, some numerical values for fixed temperatures match the Derbyshire rates. Eq. (35) is plotted in Fig. 5, where the powerful effect of CO_2 and H_2O to accelerate sintering can be seen. The activation energy of 9.9 kJ mol^{-1} is extremely low. For Omyacarb limestone under similar conditions, Adánez et al. [11] report an activation energy of 25 kJ mol^{-1}.

The prediction of sintering in the presence of CO_2 and H_2O using Borgwardt's approach, i.e. Eqs. (26), (27), (29) and (30), was tested by simulating the conditions under which Agnew et al. carried out their trials. The predicted result [35] for the initial sintering rate with $S_o = 70\ m^2\ g^{-1}$ is shown in Fig. 5. The rates have increased significantly over the nitrogen only values, and lie near the rates deduced by Agnew et al. As found by Agnew et al., there is a significant decline in apparent activation energy due to the catalytic action of the CO_2 and H_2O.

The progress of sintering using these two alternative approaches (Borgwardt and Silcox) for a limestone treated at 800 °C and atmosphere pressure in a gas containing 12% CO_2 is given in Fig. 6. The particle size is assumed to be small enough to eliminate

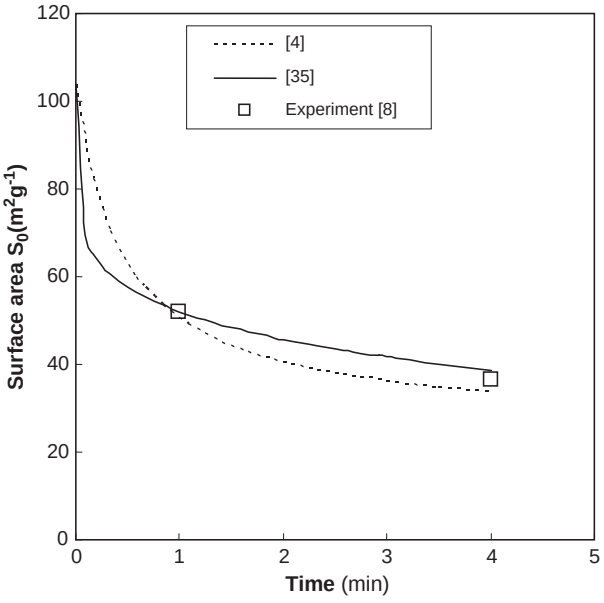

Fig. 6. The progress of sintering in lime particles under N_2 at 800 °C, as indicated by BET surface area.

transport resistances, and have an initial area of 104 $m^2\ g^{-1}$, with S_{as}=25 $m^2\ g^{-1}$. The above equations were used to calculate the values for γ and K_s, with

$$S = S_o\left(1 - (K_s t)^{\frac{1}{\gamma}}\right) \quad m^2\ g^{-1} \tag{36}$$

and Silcox's Eq. (31) integrated with time.

The results of the comparison in Fig. 6 indicate good agreement between the two approaches, and both fit the experimental points from [8]. The Borgwardt correlation is more direct and can take account of the presence of water vapour, whereas that of Silcox et al. does not. In addition, the value for the ultimate specific area is not required a priori. However, Eq. (36) predicts zero surface area at time $t=1/K_s$, and when extrapolated to infinite time an area of $-\infty$ is predicted.

3.2. Sinter properties

In addition to accelerating the sintering process, both CO_2 and H_2O cause a fall in the asymptotic surface area. Fig. 7 reproduces a figure from Mai and Edgar [23], which quantifies these values for CO_2 concentrations between 0% and 18%, and H_2O concentrations between 0% and 8%. Unfortunately they are restricted to temperatures of 1012 and 1152 °C. In all these cases, the difference in area is not great, with a range of 21 to 10 $m^2\ g^{-1}$.

The fall in porosity which results from sintering is slight after 15 min at 700 °C, but almost complete at 1100 °C [12]. Its decline with temperature follows the decline in

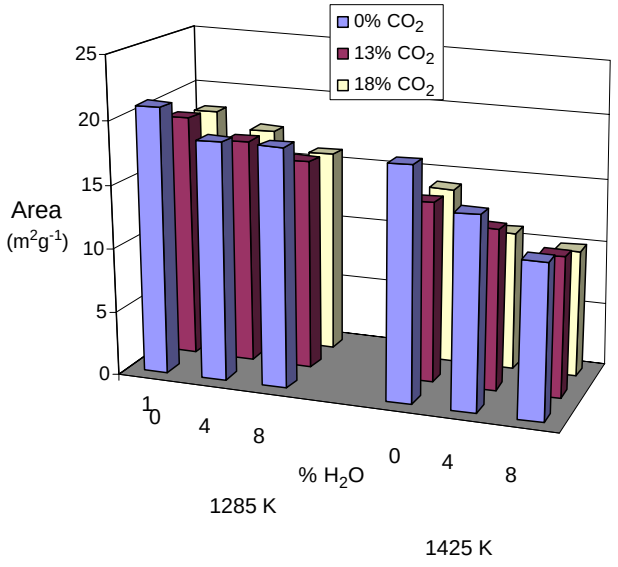

Fig. 7. The asymptotic surface areas attained by lime at two temperatures under various concentrations of CO_2 and H_2O [23].

surface area. Borgwardt identifies an initial induction period t_i during which no porosity is lost, before the intermediate shrinking stage commences. In an inert gas atmosphere, t_i is of the order of minutes at furnace temperatures. However in another paper [35] which examines sintering under atmospheres containing 12.2 kPa of CO_2 and 7.3 kPa of H_2O, he proposes times in the order of seconds.

The change in porosity during the intermediate stage of sintering was described by Borgwardt [8] with a logarithmic decline according to

$$\varepsilon_o - \varepsilon = k_p \ln(t/t_i) \tag{37}$$

Since the fall in surface area is significant during the induction time, he concludes that the loss of surface area is the predominant change affecting initial reaction rate. The plot from Borgwardt showing the effect on porosity and surface area of sintering for 15 min at various temperatures under inert gas is reproduced as Fig. 8. A more rapid response will be associated with the presence of CO_2 and H_2O.

3.2.1. Comment

All the data indicates that the onset of sintering, as determined by a fall in surface area, is greatly accelerated by the presence of CO_2 and H_2O in the gas phase. In combustion gases, the rate of shrinkage is of the order of 50 to 100 $m^2\ g^{-1}\ s^{-1}$, and is fairly insensitive to temperature over the range 700 to 1000 °C. Since the nascent area of lime is about 100 $m^2\ g^{-1}$, this means that most of the surface area changes at those temperatures will be complete in a time of the order of seconds. The predictive model of Borgwardt is the most flexible and appears to be reliable, but can be used only for short times. Particles circulating in a fluidised bed system will be extensively sintered, with surface areas likely to be between 0.1 and 1 $m^2\ g^{-1}$.

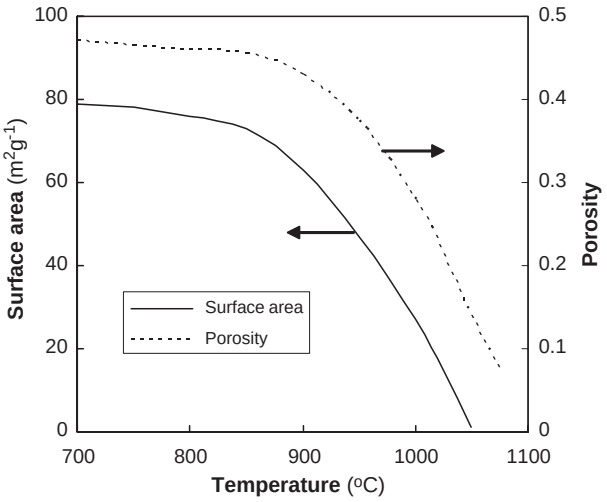

Fig. 8. The effect of temperature on the porosity and surface area of lime after 15 min exposure [8].

4. Carbonation

Carbonation is the reverse of the original calcination process, and is therefore exothermic.

$$CaO + CO_2 \rightarrow CaCO_3 \quad \Delta H = -182.1 \text{ kJ mol}^{-1}$$

Specifying the conditions for a carbonation step must strike a balance between high temperatures which favour the speed of reaction, and low temperatures which favour the equilibrium conversion.

The literature contains far more references to the process of sulphation than to carbonation. This obviously comes about because interest in the topic has been generated by the use of limestone to control SO_2 emissions. Carbonation is a much faster process than sulphation at the same temperature [5], and at 650 °C takes place rapidly. During his repeated recarbonation experiments, Barker [10] found that the carbonation reaction took place in two stages; an initial rapid rate was followed by a slower approach to a conversion plateau.

An early study of the carbonation reaction was carried out by Bhatia and Perlmutter [36]. Using a thermobalance, they calcined a limestone under atmospheres containing 0, 10 and 20% CO_2. As the concentration of CO_2 increased, the pore sizes became larger and their size distribution less spread. The crystallinity of the lime was greater for the sample prepared in pure nitrogen. Some physical properties of the calcines formed from two limestones from the USA, and of the recarbonated material are given in Table 2. All the sample particles were in the 0.71 to 0.85 mm size range, and were calcined or carbonated in a fluidised bed reactor at 750 or 850 °C for 1 h. Neither material returned to 100% conversion, i.e. totally to $CaCO_3$ under recarbonation at the comparatively high temperature of 850 °C. The 'soaking' in pure carbon dioxide at that temperature led to substantial sintering and the destruction of most of the surface area.

Abanades and Alvarez [33] examined the work on carbonation carried out by Bhatia and Perlmutter, and concluded that their findings were not only consistent with their own results, but also explained the general behaviour of calcines. Microscopy of the calcite in la Blanca limestone showed that the particles contained microcrystals with a wide range of

Table 2
Some properties of calcined and recarbonated limestones (from Krishnan and Sotirchos [9])

Limestone	State	Reaction temp. (°C)	Conversion (%)	Porosity (Hg)	Porosity (N_2)	Surface area ($m^2\ g^{-1}$)
Greer	Calcined	850	100	0.51	0.48	45
Greer	Carbonated	850	74	0.07	0.02	0.7
Georgia	Calcined	850	100	0.46	0.47	52
Georgia	Carbonated	850	56	0.03	0.01	0.3
Georgia	Recalcined	850	100	0.36	0.43	34
Greer	Calcined	750	100	0.51	0.49	56
Greer	Recalcined	750	100	0.34	0.44	27

The porosity designated (Hg) was obtained by mercury porosimetry and that marked (N_2) by nitrogen sorption.

sizes, but typically 10–20 μm in diameter. The grain structure of the parent stone remained after calcination, and the domains were recognisable even after 40 calcination/carbonation cycles. The key parameter for carbonation conversion was the fraction of porosity associated with small macropores and mesopores (<100 nm from their porosimetry data). A typical porosity value associated with these types of pores was 0.25 $cm^3\ g^{-1}$. After one calcination, the crystals of CaO are arranged in small 'rods' of about 100 nm width in parallel alignment, with pores in between.

The appearance of the same surface after 7 and 30 repeated carbonations demonstrates the progressive fusion of grains and enlargement of the pores. As the material is subjected to further cycles, the smaller pores are closed due to sintering, but the voidage tends to be retained due to the widening of the larger pores. The density of macropores increases with cycle number, and Fig. 9 of the paper of Abanades and Alvarez [33] for 30 cycles shows an open honeycomb type of structure containing pores of fairly regular size around 200 nm. However, reference to Fig. 5b of their paper (40 cycles) shows that this is not the dominant type of structure present, and there are large numbers of domains of dense, low porosity material.

Abanades and Alvarez argue that the 0.035 conversion found by Mess et al. [37] during carbonation leads to a product layer about 115 nm in thickness. They discuss the implications of this for two types of structure found in calcined limestone-clusters of small grains and the walls of mesopores. The spaces between the grains will be filled, leading to a high conversion, but there is a limited penetration into the wall material of large pores ($\approx$200 nm) over the time available for reaction. Thus as the number of grains falls, and the available surface becomes more and more restricted to larger pores, conversion will fall.

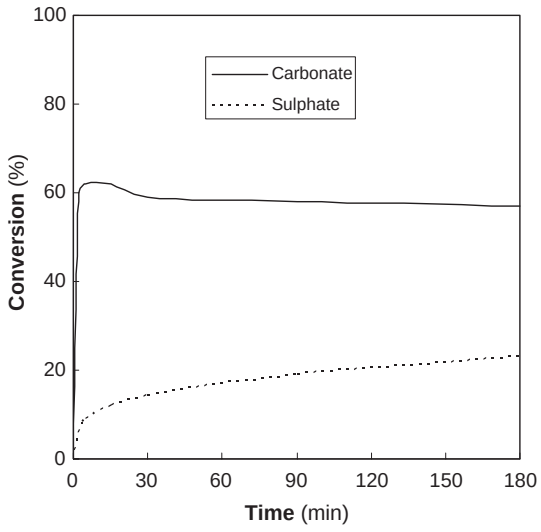

Fig. 9. The competitive conversion of lime to carbonate and sulphate in 0.3% SO_2, 70%CO_2, and 4% O_2 in nitrogen [39].

4.1. The kinetics of carbonation

It was shown by Bhatia and Perlmutter [36] that when the partial pressure of CO_2 is well below the decomposition pressure, it has little effect on rate. At temperatures between 550 and 725 °C, they identified an initiation period, followed by a growth period in carbonation, and finally a levelling off. Carbonation levels of over 70% could be obtained in a period of about 1 min for 81 and 137 μm particles. The rate of reaction was sensitive to temperature and increased as the temperature was reduced. Mass transfer effects were detected only after a significant amount of carbonation had taken place.

The carbonation over long periods of 15–20 μm particles of CaO at temperatures between 550 and 1100 °C was studied by Mess et al. [37]. After an initial rapid conversion to 0.035 in less than a minute, the rate slowed significantly. The initial crystalline grains were rounded, and about 1 μm in diameter, but grew over time to the approximate dimension of the particle. Intergranular cracking along the grain boundaries was prominent in well-carbonated samples. The slow rate period was interpreted as a parallel diffusion process, with CO_2 diffusing simultaneously down the grain boundaries and through the product crystals.

The growth of macropores in a la Blanca limestone sample was followed over a number of sintering/recarbonation cycles by Abanades et al. [33]. Calcination was carried out in a TGA at three temperatures, namely 850, 900 and 950 °C, and carbonation was carried out for 20 min at 650 °C under different partial pressures of CO_2. They claim that for all conditions, complete calcination and carbonation were achieved in a matter of minutes. Some tests were duplicated in a fixed bed reactor.

In work which was prompted by research into the effects of a meteorite strike onto carbonate minerals, Agrinier et al. [38] first calcined calcite particles of 10 μm size, and then re-reacted the evolved CO_2 with the residual calcine. This was accomplished in a reactor which was raised to 800 °C and then rapidly to 1000 °C. The elevated temperature used to ensure complete decomposition of the limestone would have produced a heavily sintered calcine, but no properties are reported. The evolved CO_2 was captured in a cold trap, and then immediately reintroduced into the reactor, which was held at temperatures between 300 and 1000 °C.

To analyse the data they adopted an empirical rate law

$$X = 1 - \exp[(-kt)^n] \tag{38}$$

and found that it fitted for the greater part of the experiment (up to 100 s at 500 °C, representing about 90% of reabsorption). The take-up of the remainder of the CO_2 was very slow. No value was given for n, and the rate expression (with the typographical error corrected) was

$$k = 7.8 \times 10^{-5} \exp(+3699/T) \quad \mathrm{s}^{-1} \tag{39}$$

which corresponds to a negative activation energy of 30 kJ mol^{-1}. Note that this relation assumes an atmosphere of 100% CO_2, so that some mechanism must be assumed in order to handle the presence of other gases.

In a practical combustor and carbonator, both the carbonation and sulphation reactions will proceed simultaneously. This problem was studied by TGA techniques [39] at a temperature of 860 °C, and at both atmospheric and elevated pressures typical of FBCs. In the atmospheric tests, Storugns limestone and pure $CaCO_3$ were first calcined in nitrogen and then reacted for different times with 0.3% SO_2, 70% CO_2, 4% O_2 and the balance nitrogen. Finally the product was recalcined in N_2 to find the amount of $CaSO_4$ formed. It was found experimentally that $CaSO_4$ did not decompose at 1133 K under nitrogen.

The behaviour of pure $CaCO_3$ and limestone showed significant differences, as the pure compound was readily sulphated at atmospheric pressure to >80% after 3 h. In contrast, the results of Iisa et al. [39] for limestone are reproduced as Fig. 9. The extent of carbonation reached a value of 60% in a matter of a minute or so, and then slowly declined over the 3 h period of the study. The reason for the sudden decline in rate is attributed to the need for CO_2 to diffuse through the newly formed product layer. At the same time, the conversion to sulphate continued to grow, indicating that some of the carbonate product was probably being converted to sulphate. The high initial rate and extent of conversion were found under unrealistically favourable conditions, with newly calcined limestone and 70% CO_2. However, the SO_2 concentration was also unrealistically high, so that in a practical situation, the competition between CO_2 and SO_2 will always favour the former.

A study of competitive carbonation and sulphation under high CO_2 concentrations was undertaken by Liu et al. [40] in the context of oxygen-enriched combustion in fluidised beds. Direct sulphation of the carbonate was found to occur.

4.1.1. Comment

In summary, the work of Abanades et al. [33] suggests that the important parameter for calcination/carbonation cycling is not the absolute values of surface area or porosity, but that associated with the grains and pores that support most of the reaction in the longer term, i.e. meso and macropores. The surface areas measured by Borgwardt using BET will not relate to the meso and macropores, because these will contribute little to surface area. The value of porosity, which responds more slowly to temperature and CO_2/H_2O, will be a better indicator. From the evolution of internal structure, Abanades concludes that the extent of carbonation is not limited by the sealing of the outer layer of the grain, but by the lack of pore space into which the crystal might grow. This supports their contention that for the short term, a limiting microporosity governs carbonation rates and extent. The rate of carbonation is much faster than sulphation, but in the longer term $CaCO_3$ will continue to be converted to $CaSO_4$.

4.2. The behaviour of calcium silicates and OCCs

Because limestone is not pure calcium carbonate, some of the common impurities and ash from a fuel can react to form other calcium compounds (OCCs) when the limestone is calcined [41]. These include calcium silicates, particularly Ca_2SiO_4 (belite or larnite), but also dicalcium ferrite $2CaO.Fe_2O_3$, calcium aluminate $CaO \cdot Al_2O_3$, calcium aluminosilicates $2CaO \cdot Al_2O_3 \cdot SiO_2$ (gehlenite) and $CaO \cdot Al_2O_3 \cdot 2SiO_2$, and calcium aluminoferrites, e.g. $4CaO \cdot Al_2O_3 \cdot Fe_2O_3$. These compounds make the calcium unavailable for

carbonation, because they react much less readily with CO_2 (and SO_2) than the parent limestone. They lower the effective capacity of the sorbent; as much as 50% of the SO_2 capacity may be lost in a CFB boiler [5]. This effect will be especially important in a system which involves recycle, such as that proposed for CO_2 sequestration.

It was found by Anthony et al. [42] that some OCCs will carbonate when hydrated and then exposed to CO_2 under pressure at near-ambient temperatures. No indication is given as to whether this will occur under the process conditions being considered here.

Kolovos et al. [43,44] reviewed the effect of foreign ions on the $CaO–SiO_2–Al_2O_3–Fe_2O_3$ system at sintering temperatures of 1200 and 1450 °C. For cations, they considered the effect on reactivity (in terms of the free CaO content, *f*CaO) caused by the addition of 1% of various metal oxides. Most of the compounds added had only a marginal effect on activity, except for CuO and Li_2O, which both produced a large decrease in *f*CaO. Copper is active even at 1100 °C, and seems to facilitate reaction between the main components. With anions at 1200 °C, Kolovos et al. [43] found that the Cl^-, F^- and SO_4^{2-} ions affect the temperature and kinetics of calcium carbonate decomposition, but no details were given. In general, anions decrease the amount of *f*CaO.

It was found by Partanen et al. [45] that the presence of small amounts of HCl will promote the formation of calcium silicate $CaSiO_3$ under fluidised bed conditions. No $CaSiO_3$ was found in the absence of HCl, which indicates that CaO and SiO_2 do not react under FBC conditions through a direct solid–solid reaction. The concentration of SO_3 in belite is 4 to 5 times that in alite, which is the more common form of silicate in cement [46]. Puertes et al. [47] report that the SO_3 in C_4A_3S (i.e. 3 CaO.3 Al_2O_3. $CaSO_4$) is more strongly held than in $CaSO_4$ itself. The compound is very stable up to 1300 °C.

4.2.1. Comment

The reported carbonation rates at 650 °C suggest that in the absence of mass transfer effects, complete conversion will be attained in less than 30 s. This indicates that most of the surface of a calcined limestone particle will initially be covered by carbonate and not sulphate crystals. The silicates and sulphates found in clinker tend to be stable in air at the temperatures under consideration.

5. Sulphation

A number of reactions may be included in the sulphation category including:

$$CaO + SO_2 + 1/2\ O_2 \rightarrow CaSO_4 \quad \Delta H = -481.4\ \text{kJ mol}^{-1}$$

$$CaCO_3 + SO_2 + 1/2\ O_2 \rightarrow CaSO_4 + CO_2 \quad \Delta H = -303\ \text{kJ mol}^{-1}$$

$$CaO + SO_2 \rightarrow CaSO_3$$

$$CaO + SO_3 \rightarrow CaSO_4$$

$$4CaO + 4SO_2 \rightarrow CaS + 3CaSO_4$$

The direct sulphation of limestone can take place if the concentration of CO_2 is above the decomposition pressure, e.g. in a pressurised system or during a recarbonation step. The magnesium oxide in a calcine will not sulphate to any appreciable extent in a FB combustion system, and the sulphation potential of OCCs is also low, see [41]. The molar volume of $CaSO_4$ is even higher than that of $CaCO_3$ (46.0 versus 36.9 cm^3 mol^{-1}), so that the problem of pore plugging is accentuated. The concept of molecular 'cramming' of the sulphate product into the constrained pore volume has been mentioned.

The literature on sulphation is extensive, and there are a number of recent reviews, namely for fluidised bed combustors by Anthony and Granatstein [5], and for high temperature pulverized fuel combustion by Cheng et al. [30]. Unfortunately many of the references in the latter review are written in the Chinese language, and most are concerned with temperatures much higher than would be considered viable for the CO_2 sequestration process. Dam-Johansen and co-authors present a series of five consecutive papers describing their extensive work on most aspects of the topic, e.g. [7,48].

5.1. Sulphate formation

The mechanism of sulphation has been examined extensively e.g [49–53]. Dennis and Hayhurst [51] used precalcined particles of Penrith limestone in a small fluidised bed, to which nitrogen containing various concentrations of SO_2 and O_2 was added. Particle sizes of 0.40, 0.78, 1.09 and 1.55 mm were studied. They concluded that SO_3 is involved and that a major pathway to the sulphate is via the sulphite $CaSO_3$. The ultimate uptakes of sulphur are decreased by an increase in the concentration of O_2, as well as by a decrease in SO_2.

Increasing the utilisation of limestone is the main focus of research into lime-based desulphurisation. In discussing the limits to sulphation, Anthony and Granatstein [5] note that limestones sulphated under oxidising conditions in the laboratory will typically attain a maximum conversion in under 90 min, and thereafter fail to react further. For example, the extent of conversion in a bubbling fluidised bed of calcined lime particles of mean diameter 390, 570 and 760 μm was found to be 26, 24 and 21% respectively [54]. In contrast, in large combustors which have very long residence times, completely converted particles have been found [41].

The previous failure of researchers to find a single criterion such as surface area or grain size by which to judge the performance of limestones under sulphation led Muñoz-Guillena et al. [50] to search for a technique more closely related to the reaction in question. They propose Temperature Programmed Reaction (TPR) in a TGA as the best guide to sulphur retention. In TPR the samples are calcined, cooled and treated with SO_2 at room temperature. The sample is then reheated at 10 K min^{-1} to 900 °C. Using 8 limestone samples, they identify those giving an SO_2 emission between 700 °C and 777 °C during TPR as the better sorbents. It was found that these samples had the lowest BET surface areas using CO_2 at 0 °C.

Working with 2–5 μm pre-calcined particles in a TGA and an entrained flow reactor, Ye et al. [29] found a two step sulphation reaction occurred in clearly defined stages. The initial step was 50% sulphation in 1–2 s, which was consistent with the filling of the available pore volume. This was interpreted as a reaction-limited step. Subsequent

reaction up to 95% conversion of CaO in 15 min was regarded as limited by diffusion through the sulphate layer. They found that a limestone from Forsby showed a higher sulphation rate after grinding than another (Ignaberga), even though the BET area of both increased. They attributed this to the higher concentration of larger pores (>5 nm) in ground Forsby limestone, which appeared to confer reactivity out of proportion to their surface area.

The initial deposits of $CaSO_4$ formed on a lime surface were found to be in the form of isolated nuclei and crystals [14]. At longer times the reaction proceeded to produce a monolayer of individual crystals with pores of 2 to 3 nm along the boundaries. At 705 °C the formation of $CaSO_4$ ceased after a few minutes at a utilisation of about 3%, whereas at 900 °C the reaction continued at a constant rate for periods of many hours. The product layer was more porous when it developed from larger stable nuclei formed during the initial reaction at higher temperatures and lower SO_2 concentrations. Liu et al. [40] report that the sulphate layer is fragile and liable to be damaged during its characterisation.

After studying the changes due to sulphation, Laursen et al. [15] noted that the grain size of nine different limestones had increased. This was not simply due to the increase in molar volume, but to agglomeration. They subjected some sulphated particles to X-ray SEM analysis for sulphur in order to identify the reaction mechanism. From the results, they proposed that three different methods of reaction were operating: (a) unreacted core (b) network and (c) uniformly sulphated. Unreacted core particles contained a highly sulphated rim, but virtually no conversion at the centre. Network particles were highly sulphated only at the periphery and along fracture lines. There was little sulphate in the portions of the grain between the fractures. Uniform particles have a homogeneous degree of sulphation (50–75%).

The stoichiometry of the sulphation reaction indicates that it should be first order with respect to SO_2 and half order with respect to oxygen. Dennis and Hayhurst [51] found that the initial rate in a fluidised bed system was pseudo first-order with respect to SO_2 when some O_2 was present. There was no recognisable influence from oxygen concentration. In contrast, many investigators, such as Ye et al. [29] report a very low order of dependence on SO_2 concentration, around 0.2 to 0.3. This is interpreted mostly as the result of a diffusional resistance through the product sulphate layer. Milne et al. [55] found an initial rapid sulphation of 7 μm Linwood calcines in less than a second, followed by a slower rate which showed a 0.6 dependence on SO_2 concentration. This applied even to high extents of conversion around 30% to 40%. The rate of reaction with respect to oxygen concentration was found to be independent of O_2 at concentrations >5%, i.e. zero order [40].

For the sulphation reaction rate, Borgwardt [12] gives

$$k_d = 2.65\ S^2 P_{SO_2}^{0.64} \exp(-36600/RT) \quad s^{-1} \tag{40}$$

The equivalent expression from Dennis and Hayhurst [51] for the initial rapid step where the rate is proportional to SO_2 concentration is:

$$k_d = 0.020_{\pm 0.015} \exp(-4570 \pm 600/T) \quad m\ s^{-1} \tag{41}$$

Li et al. [40] suggest

$$k_d = 0.977_{\pm 0.015}\exp(-65860 \pm 5000/RT) \quad \text{m s}^{-1} \tag{42}$$

Adánez et al. [56] studied the sulphation of CaO prepared from Omyacarb limestone and two types of $Ca(OH)_2$ made from it. They defined the rate constant in terms of the change in the interfacial reaction radius. This dimension, which was calculated for cylindrical or slit pores depending on the parent material, was 10 nm (diameter) and 2 nm (slit width) respectively. They derived similar diffusion coefficients for the product layer formed on lime generated from limestone and calcium hydroxide.

A comparison between the direct sulphation of limestone and the sulphation of calcines of the same material was carried out by Liu et al. [40]. They found that the rate of reaction in 80% CO_2 was almost constant up to 60% sulphation. Thus, although increased CO_2 concentrations caused lower initial rates of sulphation, the reaction rate at longer times (1 to 2 h) was higher. In addition, high CO_2 concentrations caused increased sintering of the calcined limestone, leading to the near-cessation of reaction.

5.2. Sulphate decomposition

The ability of alumina, silica and iron oxide to accelerate the decomposition of $CaSO_4$ according to:

$$CaSO_4 \rightarrow CaO + SO_2 + 1/2\ O_2$$

and to lower its decomposition temperature was noted by Fuertes and Fernandez [57]. They constructed an equilibrium phase diagram of the CaO–CaS–$CaSO_4$–SO_2–O_2 system. The corrected diagram indicates that at 1 atm total pressure and an oxygen pressure 0.03 atm, the decomposition temperature will be above 1100 °C. Specifically, at an SO_2 partial pressure of 10^{-4} atm, it is estimated to be 1140 °C. Thus there is a thermodynamic restriction on running a thermal cracker under oxidising conditions at 880 °C, and a reductant must be used. Under low oxygen conditions such as an oxygen pressure of 10^{-6} atm, CaS tends to be unstable and should revert to $CaSO_4$ at furnace temperatures. The oxidation of CaS under fluidized bed conditions has been studied by Ninomiya et al. [58].

Fuertes and Fernandez then studied the kinetics of decomposition of pure $CaSO_4$ under oxidising conditions in TGA at a range of temperatures (1057 to 1257 °C), SO_2 concentrations (0–5000 ppm) and O_2 concentrations (0–21%). The particles were needles with a mean length of 26 μm and width of 8 μm. The isothermal conversion v. time curves were found to be linear for all oxygen and sulphur dioxide concentrations. Both SO_2 and O_2 severely inhibit decomposition, and the reaction was chemically controlled. They developed a model based on an unreacted shrinking core, with an empirically derived term for gas concentrations:

$$X = \frac{2}{\rho d} k_{o1} \exp^{\frac{-E_1}{RT}} \left[\frac{1}{1 + K_{o2}\exp(-\lambda_2/RT)P_{O_2} + K_{o3}\exp(-\lambda_3/RT)P_{SO_2}} \right] t \tag{43}$$

where d is a characteristic dimension (crystal thickness for pure $CaSO_4$) The values of the parameters were fitted from the data, so that the model adequately described the effect of

gas concentration on activation energy and rate. The original paper should be consulted for the meaning of the variables and their values.

In order to identify suitable conditions for reductive decomposition of calcium sulphate, the equilibrium diagram for the CaO–CaS–$CaSO_4$–CO–SO_2 system at 850 and 950 °C was constructed by Zevenhoven et al. [59]. It shows that a concentration of only 0.1% CO is required to make CaS or CaO more stable than $CaSO_4$. At 0.01% SO_2, the favoured phase is CaO at both temperatures. Under 'slightly reducing' conditions, i.e. at a CO concentration of 0.2%, the decomposition of $CaSO_4$ to CaO was found to increase with increasing temperature.

The decomposition of sulphated samples to recover CaO by reduction with CO has been examined by Oh and Wheelock [60]. The temperature used was 1150 °C, and various ratios of CO to CO_2 were employed. If the ratio was insufficiently high, the product CaO could be slowly converted to CaS. This work was extended by Wheelock and Riel [61] in a pilot scale fluidised bed, which was operated in alternating reducing and oxidising conditions. This allowed carbon monoxide to reduce the sulphate, at the same time preventing the formation of the sulphide CaS. The feed was gypsum particles of 0.6 to 1.68 mm diameter, and the bed temperature was limited to the 1050 to 1150 °C range. At 1100 and 1150 °C under the operating conditions chosen, desulphurisation exceeded 95%, but fell to about 75% at 1050 °C.

Hansen et al. [48] point out that in a FB combustor, the solids will experience conditions which periodically change from oxidising to reducing. Under oxidising conditions the SO_2 is captured as $CaSO_4$, and under reducing conditions in the presence of CO, as CaS. From a study of 14 European limesones, a slight reduction in sulphur removal capacity is noticed under alternating oxidation and reducing conditions. Hydrogen can be used as a reductant in the place of CO, but CH_4 is not effective. Yang and Steinberg [62] propose the use of carbon in a separate kiln to reduce any sulphate formed in a coal-fired combustor.

The sulphation behaviour of three limestones under alternating oxidising and reducing conditions was studied in a quartz reactor by Mattisson and Lyngfelt [63]. The gas contained 1500 ppm of SO_2, 10% of CO_2 and either 4% O_2 or 4% CO. After 2 h of operation at 850 °C with a switch of gas composition every 60s, the conversion of Köping limestone was about 10%, that of Storugns about 20% and that of Ignaberga about 30%. It should be noted that these values were similar to those found for oxidising conditions only. The degree of conversion was sensitive to temperature, and fell as temperature was increased. For all three limestones, the conversion was lowest at 875 °C, the highest temperature used. For Köping limestone, short cycle times and operating for a greater fraction of the cycle under reducing conditions led to the lowest conversions to sulphate. The authors query the reliability of basing an industrial design on laboratory data.

A model of the operation of the performance of a limestone particle in alternating oxidising and reducing conditions was produced by Barletta et al. [64]. Unfortunately it is restricted to short time scales and is not verified by experimental results. It does suggest that the cycle time is a significant variable. During a study of the decomposition of sulphate by hydrogen, Kamphuis et al. [65] examined the reaction between CaS and Ca SO_4:

$$3/4CaSO_4 + 1/4CaS \leftrightarrow CaO + SO_2$$

They concluded that above a temperature of 830 °C there exists a two-phase mixture, consisting of the excess solid and a liquid mixture of the two compounds.

5.2.1. Comment

Although carbonation is a much faster reaction than sulphation, the literature indicates that there is a rapid initial sulphation rate of limestone calcines, followed by a slower stage limited by mass transfer. There appears to be no limitation to the conversion of active calcium over the longer term, and 100% $CaSO_4$ is realisable. This can occur despite the limitation imposed by molecular cramming. The simultaneous action of carbonation and sulphation leads to more sintering than sulphation alone. The presence of high concentrations of CO_2 initially inhibits the sulphation reaction, but in the longer term allows it to continue to greater levels of conversion.

In order to accomplish the decomposition of $CaSO_4$ at 880 °C, a reducing environment is required. This can be achieved by cycling the cracker between oxidising and reducing conditions. Greater destruction of $CaSO_4$ is achieved at higher temperatures and with frequent cycling between oxidising and reducing conditions. The most complete model for decomposition was produced under chemical control by using small crystals.

6. Particle fragmentation and attrition

The particles in a circulating bed are subject to impacts which can lead to breakage and attrition. There appears to be very little information available on fragmentation of larger limestone particles in commercial CFBs. The best data come from Scala et al. [66] who examined the problem in two ways:

1. in a small bubbling fluidised bed,
2. by impact studies when conveyed at high velocities.

The results of the attrition in the bubbling bed are similar to those presented in an earlier paper [54], which will be discussed below.

For the impact studies, 0.6–0.85 mm particles of two limestones, Massicci and Ignaberga, were prepared in different ways and then resized by screening. Some were calcined for 20 min in the fluidised bed (denoted C), others calcined (20 min) and then sulphated for 1 h (S), and others were simultaneously calcined and sulphated for 1 h (CS). They were then entrained into an air stream and propelled onto a fixed plate at velocities up to 40 m s^{-1}. The product fragments were collected and examined by light microscope and SEM.

The size distribution of the Massicci sample after calcination only (C) was similar to the feed material, but shifted to a smaller size. Since no fines were found, this was interpreted as shrinkage and rounding off of the particles. The Ignaberga stone experienced some primary fragmentation; 15% of the sample was present as fines. As noted below, the extent of attrition experienced during sulphation was much lower than for calcination.

When the Massicci samples were subjected to impact testing, the fresh limestone (F) showed the least fragmentation, whereas the C, S and CS samples all showed a much

higher loss of particles from the target size range. The losses were minor up to a velocity of 12 to 17 m s^{-1}, above which point they increased rapidly. The authors postulate a change in breakage mechanism at this point, changing from chipping to fragmentation. With the Ignaberga stone, the parent limestone behaved in a similar manner to the Massicci stone. The C and S samples had breakage patterns slightly worse than the F, while the CS material was very friable. The F, C and S Ignaberga samples exhibited a break point at the same velocity range as with Massicci, whereas the loss from the CS sample rose linearly with velocity.

Scala et al. note that two processes will lead to fragmentation (i) internal stresses due to thermal shock and the buildup of internal gas pressure (ii) rounding off of the roughness of the particle. These will be conditioned by the formation of a core–shell structure during sulphation. The first process is largely sorbent-dependent, while the second is common to all limestones. The SEM analyses of partly sulphated particles show that in each case a sulphur-rich shell of about 100 nm thickness has formed around the particles. Penetration is also achieved along pre-existing cracks.

Di Benedetto and Salatino [54] looked at the attrition of Massicci limestone particles in a small fluidised bed while the particles were being calcined and/or sulphated in a batch mode. The bed was 40 mm in diameter and was operated with a graded sand medium in the bubbling regime. The limestone contained 96.8% calcium carbonate and 2.4% magnesium carbonate. Three limestone size fractions were used: 300–425, 425–600 and 600–850 μm, with the same size of sand particle in the bed. Calcination was carried out at 850 °C using air and attrition was measured by weighing the fines which were carried out of the bed and collected in a filter. Sulphation was then carried out on the precalcined material with 1800 ppm SO_2 in 8.5% O_2 and nitrogen.

It was found that the rate of fines being elutriated from the bed fell exponentially with time during both the calcination and sulphation steps. From their graphs it is estimated that about 5% of the charge was lost during calcination, but only 0.5% during sulphation. The results confirm their supposition that CaO is more friable than $CaSO_4$; for example the fraction of $CaSO_4$ in the elutriated fines was only 15% at 30% sulphation. They conclude that the decay in the attrition rate is determined by particle round-off, so that attrition is a time-dependent rather than conversion-dependent phenomenon. Some coefficients are given to describe the attrition rates, but these would apply only to the fluid dynamic conditions of a small bubbling bed.

Experimental measurements on lime in a small pilot-scale circulating fluidised bed also found that the attrition rate decayed exponentially with time [67]. An appropriate rate correlation was developed which takes account of the fluidising conditions, the temperature, the particle concentration and the bed height. The resulting model predicts that a 0.25 mm particle will lose 9 μm in diameter after being subjected to a fluidising velocity of 7 m s^{-1} for 4000 s. This approach to estimating attrition is suitable for the sequestration systems currently under consideration.

The effect of the attrition of limestone on its ability to capture SO_2 in a pressurised fluidised bed combustor burning coal was examined by Shimizu et al. [68–70]. For addition to a large fluidised bed of 71 MW_e nominal output, the limestone was ground to <5 mm and added as a slurry. The measured rate of attrition as determined from a calcium balance on the flyash was 0.2–0.7 nm s^{-1}. The results suggest that attrition governs the

rate of SO_2 capture by the limestone; lower attrition rates lead to better solid utilisation. This conclusion was insensitive to the concentration of SO_2 in the gas.

The fragmentation of small limestone and dolostone particles under rapid heating was studied by Hu and Scaroni [71]. Particles in the 37 to 105 μm size range were heated by a laser to temperatures up to 1000 °C in under 100 ms, and the product was immediately sized by laser diffraction. They used a fracture ratio (FR) to describe the extent of fragmentation:

$$\mathrm{FR} = \frac{\text{volume of median particles after heating}}{\text{volume of median particles before heating}}$$

Dolostones were far more likely to break, probably because of the more rapid decomposition of $MgCO_3$ compared to $CaCO_3$. Significant breakage of the most friable sample did not occur at temperatures below 650 °C. The extent of calcination, even up to 60% did not lead to significant extra breakage of the five true limestones.

6.1. Summary

Particles circulating through two fluidised beds will rapidly suffer attrition and be rounded off. After this initial shaping, attrition should be minimal, except if cracks appear in the particles as the result of molecular cramming. Since the raw limestone is stronger than its products, a recarbonated particle is probably only slightly weaker than its parent. Any sulphation products remaining on the surface will add to the strength. The measured attrition rate in a PFBC of about 2 μm in diameter per hour [68] should apply to an atmospheric bed if the velocities in both beds are similar. One can conclude that very little breakage of calcined, partly recarbonated particles should occur, unless the break point velocity of 12 to 15 m s^{-1} is exceeded.

7. Application to CO_2 sequestration in circulating fluidised beds

The possibility of using the calcination/carbonation cycle to sequester the carbon dioxide formed in thermal processes has been proposed by a number of researchers e.g [2,3,10]. A pair of circulating fluidised beds (CFB) has been seen a good system to accomplish this task.

Long residence times are reported in a 40 MW CFB by Anthony and Granatstein [5]. The major fraction of the sorbent (80–85%) had a residence of an hour or more (with a peak of 32 h). The mean residence times of commercial boilers were found to approach 10 h. As a result, they caution against placing too much weight on results obtained in laboratory systems, which are difficult to operate in a manner which simulates large CFBs. This is especially so in relation to alternating oxidising/reducing conditions, although long residence times will tend to negate these effects.

Abanades and coworkers have published several papers examining this system, employing sequential calcination and regeneration steps [2,33,72]. They report that the capacity of limestone to be recarbonated falls continuously with the sequence of cycles. After examining data from a number of researchers who used different limestones,

different particle sizes (10 μm to 10 mm) and a range of treatment temperatures (750 to 1060 °C), they concluded that the uniformity in conversion displayed by equivalent data permits a generalised correlation to be adopted.

The exceptions to the conclusion by Abanades et al. that all limestones behave similarly are some of their collected data for severe sintering conditions, notably by Deutch for 1270 °C and 1 atm of CO_2, and their own tests at 950 °C and 1 atm CO_2. In both these cases the conversion capacity was significantly lowered in comparison to the bulk of the data. It should also be noted that some data by Barker [10] are included in this synthesis. Barker reports his results for 40×24 h cycles at 866 °C using pure $CaCO_3$. The unified fall in conversion capability reported by Abanades applies to $CaCO_3$ contents measured after the initial short-term carbonation step noted by Barker. If the longer term conversion reported by Barker over 24 h is used, the utilisation of the lime would be much higher than proposed by Abanades.

The correlation relating the conversion capacity to the number of the cycle is given as

$$X_N = f_m^N (1 - f_w) + f_w$$

where N is the number of the cycle (for uncalcinated limestone $N=0$), and f_m is the fractional loss in conversion from the previous cycle, assumed constant with N. The parameter f_w is the theoretical residual capacity after infinite cycles, and is determined by several factors including the structure of the calcine and the thickness of the product layer. From their collection of data, Abanades and Alvarez [33] assign a value of 0.77 to f_m and 0.17 to f_w.

7.1. Modelling the process

In order to simulate the performance of a lime sequestration system, it would be necessary to develop a suitable process model. This model would combine the aerodynamics and trajectories of particles circulating in the fluidised beds with a description of the changes induced by the various reactions of the lime under process conditions. The behaviour of fluidised beds has received considerable attention, but there appears to be less information about limestone performance in this environment. The model of Li et al. [67] has taken some steps in this direction. Some of the reaction models examined in this review are based on conflicting assumptions.

The various approaches to modelling the processes of calcination, carbonation and sulphation are summarised below. Sintering has been discussed above and is not included. There are three major groups of models, which focus either on the voids in the particle (pores), or the solid phase (grains), or the progress of a reaction through a homogeneous particle. Each group consists of the first formulation and subsequent refinements of the details. They describe the structure of the porous particle, and the way that the structure changes during a gas–solid reaction.

All the models must include the diffusion of reactant or product gas through the internal voids [9,37,73,74]. The mechanism of diffusion may be molecular diffusion in large pores ($\approx 10^{-4}$ m^2 s^{-1} in magnitude), Knudsen diffusion in micropores ($\approx 10^{-6}$ m^2 s^{-1}), or may be movement through a layer of product carbonate or sulphate ($\approx 10^{-11\text{–}13}$ $m^2 s^{-1}$). There

is a considerable range of values presented for the latter, probably because of mechanical defects in the product layer, such as cracks at grain boundaries [37]. Adánez et al. [56] showed that a great difference in results was produced for Knudsen diffusion, depending on whether the pores were regarded as cylindrical or slit-shaped.

7.1.1. Random pore model (RPM)

The RPM was developed and first applied by Bhatia and Perlmutter [75] to the sulphation of lime. The pores are regarded as a series of uniform diameter, randomly oriented cylinders which initially overlap. As the reaction proceeds in a situation where the solid is consumed and lost as a gaseous product, the pores grow in diameter and the surface area rises to a maximum before falling to zero. The distributed pore size model (DPSM) allows for a distributed pore size distribution rather than using a single pore size.

7.1.2. Grain model

In this model, a particle is regarded as an assembly of small spherical grains, such that the voids between them are responsible for microporosity. The changing grain size model (CGSM) described by García-Labiano et al. [13] and Adanez et al. [56] combines the grain and shrinking core approaches. As the reaction proceeds through the assembly of identical spherical grains, the grain size grows while the unreacted core shrinks. A similar physical system is proposed by Ghosh-Dastidar et al. [24] and Muhali [76]. Milne et al. extended this concept to accommodate sintering by allowing the spherical grains to overlap by fusion [77]. As Murthy et al. [32] used large cylindrical compacts of fine powder, the grain model was appropriate for this system.

7.1.3. Homogeneous particle model (HPM)

The simplest example of this approach is the shrinking core model (SCM), which has a very long history, and can be shown to apply in certain cases of calcination, e.g. Blanca limestone [13]. It was also adopted by Silcox et al. [4] for this purpose. Hu and Scaroni [22] and Khinast et al. [21] considered that the heat and mass transfer processes within the particle would produce a radial conversion profile within all but the smallest particles. They applied classical theory for porous media to these effects in order to predict conversion (see for example Fig. 7).

Adanez et al. [11] criticised the previous modelling endeavours on the basis that an insufficient number of values of some variables was included in the experimental verification tests. This applied particularly to the number of types of limestone and the particle sizes used. Accordingly, they set up a program involving seven different limestones and seven particle sizes with mean diameters ranging from 158 to 1788 μm. The behaviour of their calcines during sulphation was then studied at one temperature (850 °C) and one SO_2 concentration (2500 ppm).

The data obtained were used to test three models—namely the CGSM, the RPM and the DPSM. It was found that the CGSM and RPM were not able to adequately predict the sulphation conversion versus time curves for all cases. The DPSM fared better when applied to calcines with a broad range of pore sizes, provided the product layer diffusion coefficient and the tortuosity were used as fitting parameters. For limestones with a

Table 3
Comparison of CO_2 sequestration costs (US dollars)

Detail	Electricity generation		Cost of avoided CO_2 ($/t)[a]	Reference
	% Penalty in efficiency	Comparative[b] costs (c/kW h)		
Electricity/MEA	8–13	×2	70–90	[79]
Electricity/MEA	27	4.9→9.7	59	[80]
Electricity/MEA	21	4.3→6.9	40+	[81]
Utilisation			0–20	[82]
Oil recovery			35–160	
Storage			90–280	
Geologic storage			110–330	
Ocean storage			110–330	

[a] All costs except those of Herzog and Vukmirovic [81] and utilisation under Grimston et al. [82] include compression and pipelining 100 to 300 km for storage or disposal.
[b] The two figures represent power generated without and with CO_2 sequestration.

uniform pore size distribution, which is usually the case, the above two parameters had to be modified for each particle size.

7.2. Economics

The costs for sequestering CO_2 have become a topic of considerable interest to governments; for example to the USDOE [78] and the European community (Document L 275/32, 2003). Comparison of the various techniques is difficult, given the vastly different fundamental energy generation systems in service, and the range of possible sequestration techniques. Another complication is the different basis for carrying out economic analyses.

Table 3 lists some of the figures quoted for CO_2 sequestration, mostly involving extraction from the flue gas stream by absorption into amines. The figures given by Sims et al. [79], Rao and Rubin [80], and Herzog and Vukmirovic [81] are the result of studies of conventional electricity generating stations fired with fossil fuels and fitted with methyl ethylamine (MEA) absorbers. The figure given by Herzog does not include compression and pipelining costs. All the estimates indicate that the cost of power will effectively double, and the cost of avoided CO_2 will be >US$60 per tonne.

The values in Table 3 given by Grimston et al. [82] are collected from a range of sources and cover general categories. Obviously, when the CO_2 can be utilised on-site, the costs are lower than when compression and transmission are required. The preparation of a disposal site will add to the costs of the project. In general, the costs are higher than those estimated from specific studies of power generation.

Acknowledgements

We thank ALSTOM, CEMEX and ADEME for their financial support of this work. We also thank Ms. Beal, M. Morin (ALSTOM) and M. Roeder (CEMEX) for fruitful discussions.

References

[1] P. Freund, International collaboration on capture, storage and utilisation of greenhouse gases, Waste Manage. 17 (1997) 281–287.

[2] J.C. Abanades, D. Alvarez, E.J. Anthony, D. Lu, In-situ capture of CO_2 in a fluidized bed combustor, Proc. 17th Int. Fluidized Bed Combustion Conference, Jacksonville Florida, May 2003.

[3] C. Salvador, D. Lu, E.J. Anthony, J.C. Abanades, Enhancement of CaO for CO_2 capture in an FBC environment, Chem. Eng. J. 96 (2003) 187–195.

[4] G.D. Silcox, J.C. Kramlich, D.W. Pershing, A mathematical model for the flash calcination of dispersed $CaCO_3$ and $Ca(OH)_2$ particles, Ind. Eng. Chem. Res. 28 (1989) 155–160.

[5] E.J. Anthony, D.L. Granatstein, Sulphation phenomena in fluidized bed combustion systems, Prog. Energy Combust. Sci. 27 (2001) 215–236.

[6] A. Trikkel, Estonian calcareous rocks and oil shale ash as sorbents for SO_2, PhD thesis, Tallinn Technical University, 2001.

[7] K. Dam-Johansen, K. Østergaard, High temperature reaction between sulphur dioxide and limestone—I. Comparison of limestones in two laboratory reactors and a pilot plant, Chem. Eng. Sci. 46 (1991) 827–837.

[8] R.H. Borgwardt, Sintering of nascent calcium oxide, Chem. Eng. Sci. 44 (1989) 53–60.

[9] S.V. Krishnan, S.V. Sotirchos, Effective diffusivity changes during calcination, carbonation, recalcination and sulfation of limestones, Chem. Eng. Sci. 49 (1994) 1195–1208.

[10] R. Barker, The reversibility of the reaction $CaCO_3 \leftrightarrow CaO + CO_2$, J. Appl. Chem. Biotechnol. 23 (1973) 733–742.

[11] J. Adánez, P. Gayán, F. García-Labiano, Comparison of mechanistic models for the sulfation reaction in a broad range of particle sizes of sorbents, Ind. Eng. Chem. Res. 35 (1996) 2190–2197.

[12] R.H. Borgwardt, N.F. Roache, K.R. Bruce, Method for variation of grain size in studies of gas–solid reactions involving CaO, Ind. Eng. Chem. Fundam. 25 (1986) 165–169.

[13] F. García-Labiano, A. Abad, L.F. de Diego, P. Gayán, J. Adánez, Calcination of calcium-based sorbents at pressure in a broad range of CO_2 concentrations, Chem. Eng. Sci. 57 (2002) 2381–2393.

[14] W. Duo, K. Laursen, J. Lim, J. Grace, Crystallisation and facture: formation of product layers in sulfation of calcined limestone, Powder Technol. 111 (2000) 154–167.

[15] K. Laursen, W. Duo, J.R. Grace, J. Lim, Sulfation and reactivation characteristics of nine limestones, Fuel 79 (2000) 153–163.

[16] J.-M. Huang, K.E. Daugherty, Lithium carbonate enhancement of the calcination of calcium carbonate: proposed extended-shell model, Thermochim. Acta 118 (1987) 135–141.

[17] J.-M. Huang, K.E. Daugherty, Inhibition of the calcination of calcium carbonate, Thermochim. Acta 130 (1988) 173–176.

[18] Q. Zhong, I. Bjerle, Calcination kinetics of limestone and the microstructure of nascent CaO, Thermochim. Acta 223 (1993) 109–120.

[19] J.S. Dennis, A.N. Hayhurst, Mechanism of the sulphation of calcined limestone particles in combustion gases, Chem. Eng. Sci. 45 (1990) 1175–1187.

[20] C.R. Milne, G.D. Silcox, D.W. Pershing, D.A. Kirchgessner, Calcination and sintering models for application to high-temperature, short-time sulfation of calcium-based sorbents, Ind. Eng. Chem. Res. 29 (1990) 139–149.

[21] J. Khinast, G.F. Krammer, Ch. Brunner, G. Staudinger, Decomposition of limestone: the influence of CO_2 and particle size on the reaction rate, Chem. Eng. Sci. 51 (1996) 623–634.

[22] N. Hu, A.W. Scaroni, Calcination of pulverised limestone particles under furnace injection conditions, Fuel 75 (1996) 177–186.

[23] M.C. Mai, T.F. Edgar, Surface area evolution of calcium hydroxide during calcination and sintering, AIChE J. 35 (1989) 30–36.

[24] A. Ghosh-Dastidar, S.K. Muhali, R. Agnihotri, L.-S. Fan, Ultrafast calcination and sintering of $Ca(OH)_2$ powder: experimental and modeling, Chem. Eng. Sci. 50 (1995) 2029–2040.

[25] J.S. Dennis, A.N. Hayhurst, The effect of temperature on the kinetics and extent of SO_2 uptake by calcareous materials during fluidised bed combustion, Proc. 20th Symposium (Int) on Combustion, the Combustion Institute, 1984, pp. 1347–1355.

[26] T. Darroudi, A.W. Searcy, Effect of CO_2 pressure on the rate of decomposition of calcite, J. Phys. Chem. 85 (1981) 3971–3974.
[27] Y. Wang, W.J. Thomson, The effects of steam and carbon dioxide on calcite decomposition using dynamic X-ray diffraction, Chem. Eng. Sci. 50 (1995) 1373–1382.
[28] J. Agnew, E. Hampartsoumian, J.M. Jones, W. Nimmo, The simultaneous calcination and sintering of calcium based sorbents under a combustion atmosphere, Fuel 79 (2000) 1515–1523.
[29] Z. Ye, W. Wang, Q. Zhong, I. Bjerle, High temperature desulfurisation using fine sorbent particles under boiler injection conditions, Fuel 74 (1995) 743–750.
[30] J. Cheng, J. Zhou, L. Jiu, Z. Zhou, Z. Huang, X. Cao, X. Zhao, K. Cen, Sulfur removal at high temperature during coal combustion in furnaces: a review, Prog. Energy Combust. Sci. 29 (2003) 381–405.
[31] A. Ghosh-Dastidar, S.K. Muhali, R. Agnihotri, L.-S. Fan, Investigation of high-reactivity calcium carbonate sorbent for enhanced SO_2 capture, Ind. Eng. Chem. Res. 35 (1996) 598–606.
[32] M.S. Murthy, B.R. Harish, K.S. Rajanandam, K.Y. Ajoy Pavan Kumar, Investigation on the kinetics of thermal decomposition of calcium carbonate, Chem. Eng. Sci. 49 (1994) 2198–2204.
[33] J.C. Abanades, D. Alvarez, Conversion limits in the reaction of CO_2 with lime, Energy Fuels 17 (2003) 308–315.
[34] R.M. German, Z.A. Munir, Surface area reduction during isothermal sintering, J. Am. Ceram. Soc. 59 (1976) 379–383.
[35] R.H. Borgwardt, Calcium oxide sintering in atmospheres containing water and carbon dioxide, Ind. Eng. Chem. Res. 28 (1989) 493–500.
[36] S.K. Bhatia, D.D. Perlmutter, The effect of product layer on the kinetics of the CO_2-lime reaction, AIChE J. 29 (1983) 79.
[37] D. Mess, A.F. Sarofim, J.P. Longwell, Product layer diffusion during the reaction of calcium oxide with carbon dioxide, Energy Fuels 13 (1999) 999–1005.
[38] P. Agrinier, A. Deutsch, U. Schärer, I. Martinez, Fast back-reactions of shock-released CO_2 from carbonates: an experimental approach, Geochim. Cosmochim. Acta 65 (2001) 2615–2632.
[39] K. Iisa, C. Tullin, M. Hupa, Simultaneous sulfation and recarbonation of calcined limestone under PFBC conditions, Proc. 11th Int. Conf. Fluidised bed Comb., ASME, 1991, pp. 83–90.
[40] H. Liu, S. Katagiri, U. Kaneko, K. Okazaki, Sulfation behavior of limestone under high CO_2 concentration in O_2/CO_2 coal combustion, Fuel 79 (2000) 945–953.
[41] E.J. Anthony, A.P. Iribarne, J.V. Iribarne, L. Jia, Reuse of landfilled FBC residues, Fuel 76 (1997) 603–606.
[42] E.J. Anthony, L. Jia, J. Woods, W. Roque, S. Burwell, Pacification of high calcic residues using carbon dioxide, Waste Manage. 20 (2000) 1–13.
[43] K. Kolovos, P. Loutsi, S. Tsivilis, G. Kakali, The effect of foreign ions on the reactivity of the $CaO–SiO_2–Al_2O_3–Fe_2O_3$ system Part I. Anions, Cem. Concr. Res. 31 (2001) 425–429.
[44] K. Kolovos, S. Tsivilis, G. Kakali, The effect of foreign ions on the reactivity of the $CaO–SiO_2–Al_2O_3–Fe_2O_3$ system Part II: Cations, Cem. Concr. Res. 32 (2002) 463–469.
[45] J. Partanen, P. Backman, M. Hupa, The effect of HCl on the formation of calcium silicates in sand beds in fluidized bed boilers, Combust. Flame 130 (2002) 376–380.
[46] H.F.W. Taylor, Distribution of sulphate between phases in Portland cement clinker, Cem. Concr. Res. 29 (1999) 1173–1179.
[47] F. Puertas, M.T. Blanco Varela, S. Giménez Molina, Kinetics of the thermal decomposition of C_4A_3S in air, Cem. Concr. Res. 25 (1995) 572–580.
[48] P.F.B. Hansen, K. Dam-Johansen, K. Østergaard, High temperature reaction between sulphur dioxide and limestone—V. The effect of periodically changing oxidising and reducing conditions, Chem. Eng. Sci., 48, 1993, pp. 1325–1341.
[49] M.J. Muñoz-Guillena, A. Linares-Solano, C. Salinas-Martínez de Lecea, A study of $CaO–SO_2$ interaction, Appl. Surf. Sci. 81 (1994) 409–415.
[50] M.J. Muñoz-Guillena, A. Linares-Solano, C. Salinas-Martínez de Lecea, High temperature SO_2 retention by CaO, Appl. Surf. Sci. 99 (1996) 111–117.
[51] J.S. Dennis, A.N. Hayhurst, The effect of CO_2 on the kinetics and extent of calcination of limestone and dolomite particles in fluidised beds, Chem. Eng. Sci. 42 (1987) 2361–2372.

[52] G.J. Zijlma, A.W. Geritsen, C.M. van den Bleek, SO_2 retention in fluidized bed combustors, modelling and influence of oxygen, Proc. 15th Int. Conf. Fluidized Bed Comb., Savannah, May 1999.
[53] R. Zevenhoven, P. Yrjas, M. Hupa, Sulfur dioxide capture under PFBC conditions: the influence of sorbent particle structure, Fuel 77 (1998) 285–292.
[54] A. Di Benedetto, P. Salatino, Modelling attrition of limestone during calcination and sulfation in a fluidized bed reactor, Powder Technol. 95 (1998) 119–128.
[55] C.R. Milne, G.D. Silcox, D.W. Pershing, D.A. Kirchgessner, High-temperature, short-time sulfation of calcium-based sorbents: 1. Theoretical sulfation model, Ind. Eng. Chem. Res. 29 (1990) 2192–2201.
[56] J. Adánez, F. García-Labiano, V. Fierro, Modelling for the high-temperature sulphation of calcium-based sorbents with cylindrical and plate-like pore geometries, Chem. Eng. Sci. 55 (2000) 3665–3683.
[57] A.B. Fuertes, M.J. Fernandez, Kinetics of the calcium sulphate decomposition, Trans. Inst. Chem. Eng. 73 (1995) 854–862 (Part A).
[58] Y. Ninomiya, Z.-B. Dong, M. Iijima, A. Sato, Oxidation mechanism of calcium sulfide sorbent, 15th Int. Conf. Fluidised Bed Comb., Savannah 1999.
[59] R. Zevenhoven, P. Yrjas, M. Hupa, Sulfur capture under periodically changing oxidising and reducing conditions in PFBC, 15th Int. Conf. Fluidised Bed Comb., Savannah 1999.
[60] J.S. Oh, T.D. Wheelock, Reductive decomposition of calcium sulphate with carbon monoxide: Reaction mechanism, Ind. Eng. Chem. Res. 29 (1990) 544–550.
[61] T.D. Wheelock, T. Riel, Cyclic operation of a fluidized bed reactor for decomposing calcium sulfate, Chem. Eng. Commun. 109 (1991) 155–166.
[62] R.T. Yang, M. Steinberg, Regeneration of lime from sulfates for fluidized-bed combustion, US Patent 4,197,285, April, 1980.
[63] T. Mattisson, A. Lyngfelt, The reaction between limestone and SO_2 under periodically changing oxidising and reducing conditions—effect of temperature and limestone type, Thermochim. Acta 325 (1999) 59–67.
[64] D. Barletta, A. Marzocchella, P. Salatino, Modelling the SO_2-limestone reaction under periodically changing oxidizing/reducing conditions: the influence of cycle time on reaction rate, Chem. Eng. Sci. 57 (2002) 631–641.
[65] B. Kamphuis, A.W. Potma, W. Prins, W.P.M. Van Swaij, The reductive decomposition of calcium sulphate—I. Kinetics of the apparent solid–solid reaction, Chem. Eng. Sci. 48 (1993) 105–116.
[66] F. Scala, P. Salatino, R. Boerefijn, M. Ghadiri, Attrition of sorbents during fluidized bed calcination and sulphation, Powder Technol. 107 (2000) 153–167.
[67] X. Li, Z. Luo, M. Ni, K. Cen, Modeling sulfur retention in circulating fluidized bed combustors, Chem. Eng. Sci. 50 (1995) 2235–2242.
[68] T. Shimizu, P. Meglow, S. Sakuno, N. Misawa, N. Suzuki, H. Ueda, H. Sasatsu, H. Gotou, Effect of attrition on SO_2 capture by limestone under pressurised fluidized bed combustion conditions—comparison between a mathematical model of SO_2 capture by single limestone particle under attrition condition and SO_2 capture in a large-scale PFBC, Chem. Eng. Sci. 56 (2001) 6719–6728.
[69] T. Shimizu, M. Peglow, K. Yamagiwa, M. Tanaka, S. Sakuno, N. Misawa, N. Suzuki, H. Ueda, H. Sasatsu, H. Gotou, A simplified model for SO_2 capture by limestone in 71 MWe pressurised fluidized bed combustor, Chem. Eng. Sci. 57 (2002) 4117–4128.
[70] T. Shimizu, M. Peglow, K. Yamagiwa, M. Tanaka, Comparison among attrition-reaction models of SO_2 capture by uncalcined limestone under pressurized fluidized bed conditions, Chem. Eng. Sci. 58 (2003) 3053–3057.
[71] N. Hu, A.W. Scaroni, Fragmentation of calcium-based sorbents under high heating rate, short residence time conditions, Fuel 74 (1995) 374–382.
[72] J.C. Abanades, The maximum capture efficiency of CO_2 using a carbonation/calcination cycle of CaO/$CaCO_3$, Chem. Eng. J. 90 (2002) 303–306.
[73] F.R. Campbell, A.W.D. Hills, A. Paulin, Transport properties of porous lime and their influence on the decomposition of porous compacts of calcium carbonate, Chem. Eng. Sci. 25 (1970) 929–942.
[74] J.Y. Xie, B.J. Zhong, W.B. Fu, Y. Shi, Measurement of equivalent diffusivity during the calcination of limestone, Combust. Flame 129 (2002) 351–355.

[75] S.K. Bhatia, D.D. Perlmutter, The effect of pore structure on fluid–solid reactions: application to the SO_2-lime reaction, AIChE J. 27 (1981) 226–234.
[76] S.K. Mahuli, R. Agnihotr, R. Jadhav, S. Chauk, L.-S. Fan, Combined calcination, sintering and sulphation model for $CaCO_3$–SO_2 reaction, AIChE J. 45 (1999) 367–382.
[77] C.R. Milne, G.D. Silcox, D.W. Pershing, D.A. Kirchgessner, High-temperature, short-time sulfation of calcium-based sorbents: 2. Experimental data and theoretical model predictions, Ind. Eng. Chem. Res. 29 (1990) 2201–2214.
[78] S.M. Klara, R.D. Srivastava, H.G. McIlvried, Integrated collaborative technology development for CO_2 sequestration in geologic formations—United States Department of Energy R&D, Energy Convers. Manag. 44 (2003) 2699–2712.
[79] R.E.H. Sims, H.-H. Rogner, K. Gregory, Carbon emission and mitigation cost comparisons between fossil fuel, nuclear and renewable energy resources for electricity generation, Energy Policy 31 (2003) 1315–1326.
[80] A.B. Rao, E.S. Rubin, A technical, economic and environmental assessment of amine-based CO_2 capture technology for power plant greenhouse control, Environ. Sci. Technol. 36 (2002) 4467–4475.
[81] H.J. Herzog, N. Vukmirovic, CO_2 sequestration: opportunities and challenges, Proc. 7th Clean Coal Technol. Conf., Knoxville, June 1999.
[82] M.C. Grimston, V. Karakoussis, F. Rouquet, R. van der Vorst, P. Pearson, M. Leach, Review. The European and global potential of carbon dioxide sequestration in tackling climate change, Clim. Policy 1 (2001) 155–171.
[83] N. Benhidjeb, R. Gadiou, J.-F. Brilhac, G. Prado, Modelling of the pore sulphation behaviour of porous CaO particles in a fixed bed reactor, Environ. Comb. Technol. 2 (2001) 255–275.